High resolution in-vitro and in-vivo X-ray micro-CT imaging using synchrotron radiation

Alberto Bravin

ID17 Biomedical Beamline

European Synchrotron Radiation Facility (Grenoble, France)

bravin@esrf.fr

Dubrovnik – 22 October 2018

OUTLINE

- **Looking in inside biological samples in 3D: tomography**

- **Absorption contrast and phase contrast: a magic team. Applications in neuroimaging**

- **Synchrotrons and synchrotron radiation**

FROM THE X-RAYS DISCOVERY TO SYNCHROTRON RADIATION

Getty Archives

’70 Housfield CT machine

Hospital CT machine

1895?

60ies

Clinics

today

Research

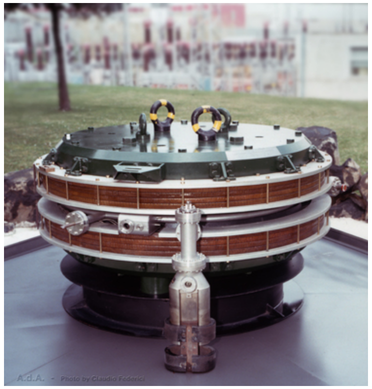

AdA, INFN, Rome

SR: Largest X-ray source

Contrast type		Information
Absorption radiography Phase contrast radiography	→	Morphology/Functioning
Fluorescence	→	Composition
Small angle scattering Diffraction	→	Structure
EXAFS/XANES	→	Chemical state

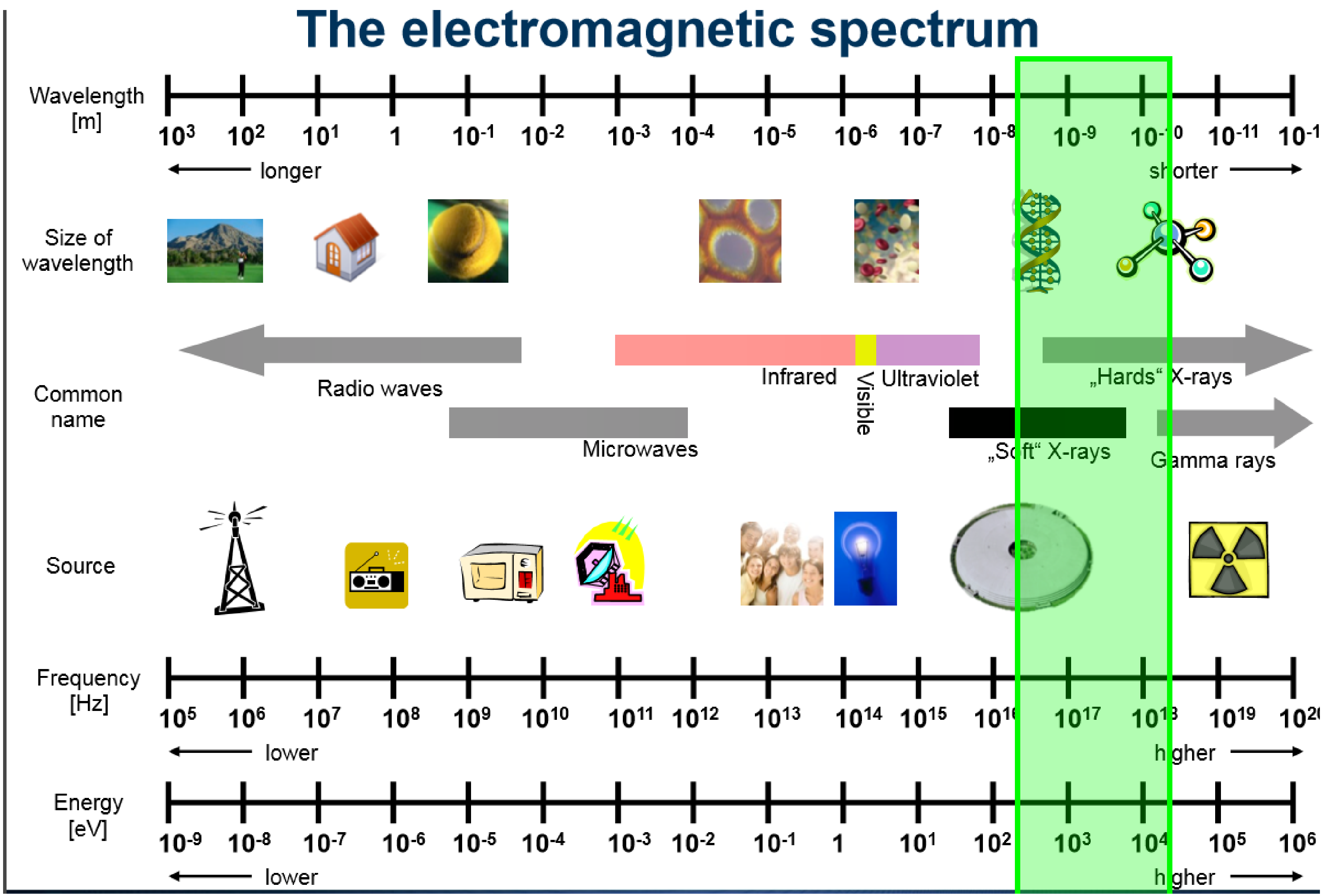

The electromagnetic spectrum
Wavelength [m]
10^3 10^2 10^1 1 10^-1 10^-2 10^-3 10^-4 10^-5 10^-6 10^-7 10^-8 10^-9 10^-10 10^-11
longer
shorter
Size of wavelength
Common name
Radio waves
Microwaves
Infrared
Visible
Ultraviolet
„Soft" X-rays
„Hards" X-rays
Gamma rays
Source
Frequency [Hz]
10^5 10^6 10^7 10^8 10^9 10^10 10^11 10^12 10^13 10^14 10^15 10^17 10^19
lower
higher
Energy [eV]
10^-9 10^-8 10^-7 10^-6 10^-5 10^-4 10^-3 10^-2 10^-1 1 10^1 10^2 10^3 10^4 10^5 10^6
lower
higher

X-RAY RADIOGRAPHY: PRINCIPLE

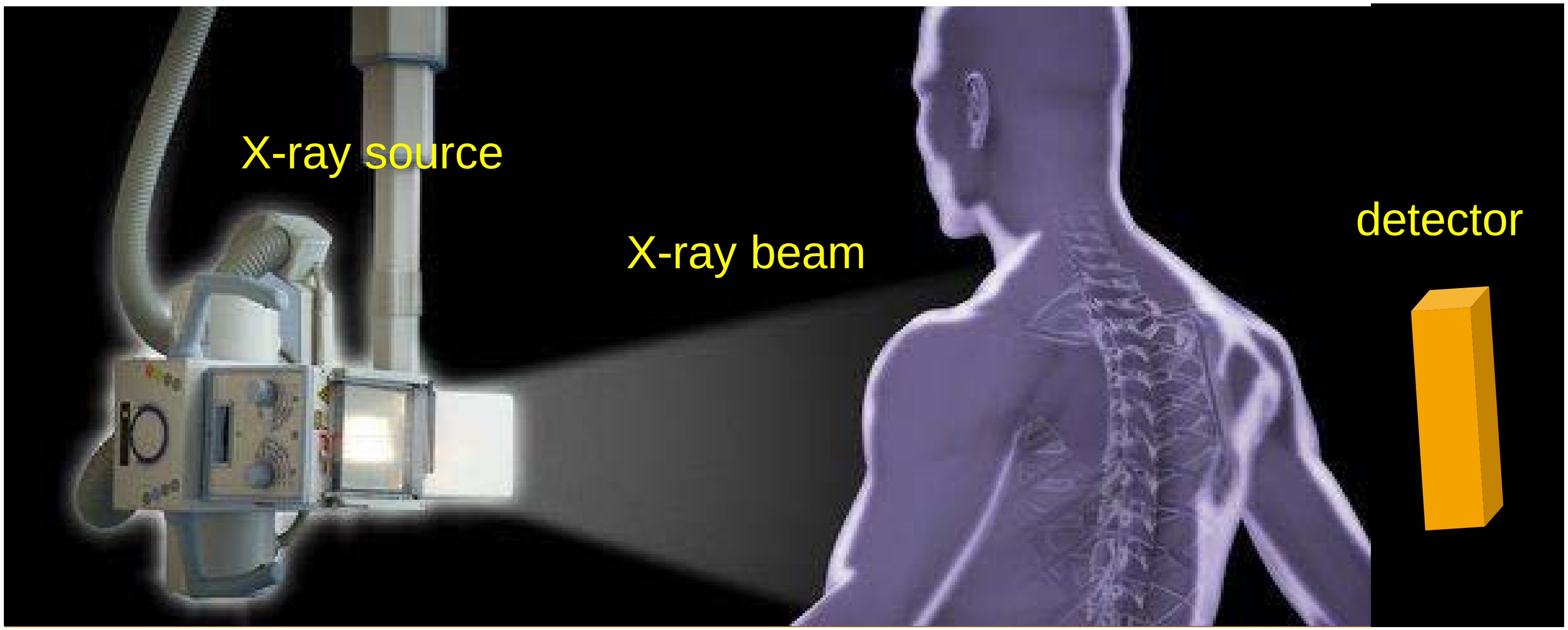

X-ray absorption imaging $I = I_0 \exp(-\mu x)$ *Beer-Lambert law*

Image: a map of the differential absorption of X-rays by the tissues

Bone (Ca): high absorption, high contrast
Soft tissues (H, O, C, N): low absorption, low contrast

LIMITS OF X-RAY RADIOGRAPHY

Mammography

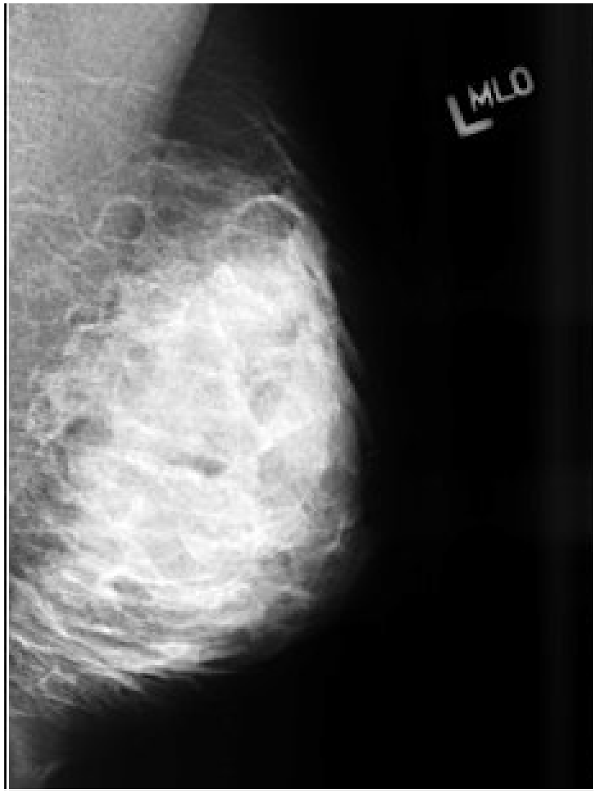

Tumors in dense (glandular) breasts
are masked by tissues

Bone and cartilage

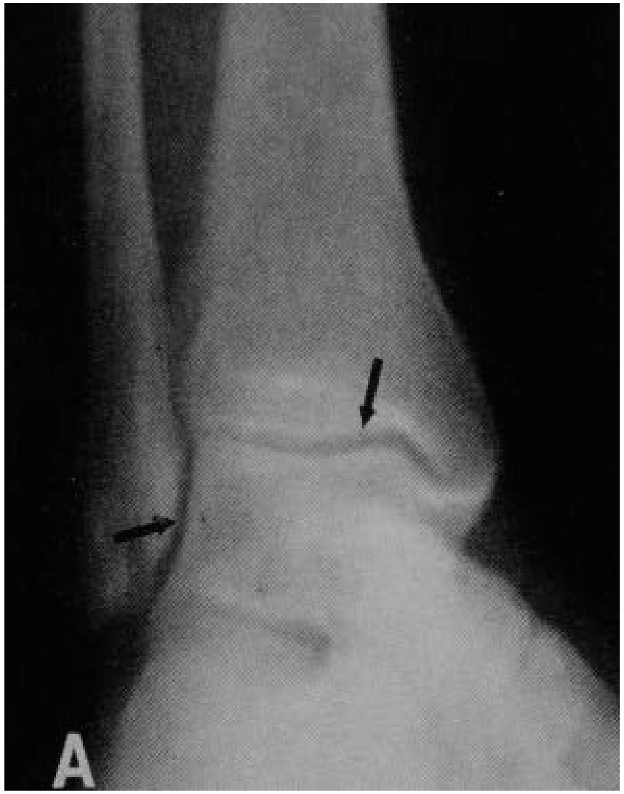

Cartilage (low density) in between
Bones are invisible

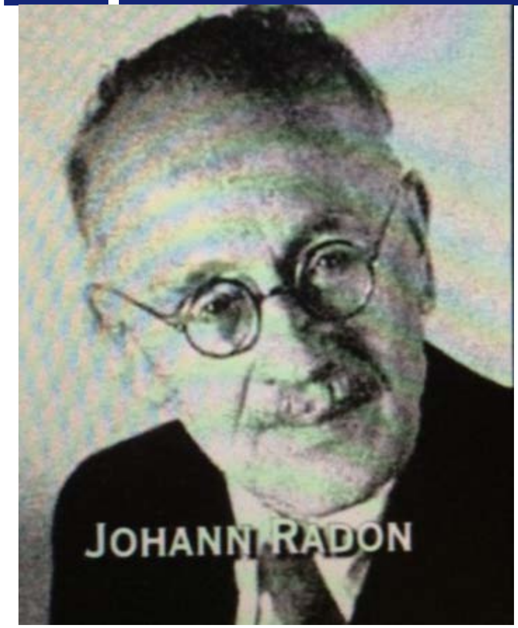

Radon 1917

EMI-Beatles

The development of computing technologies by

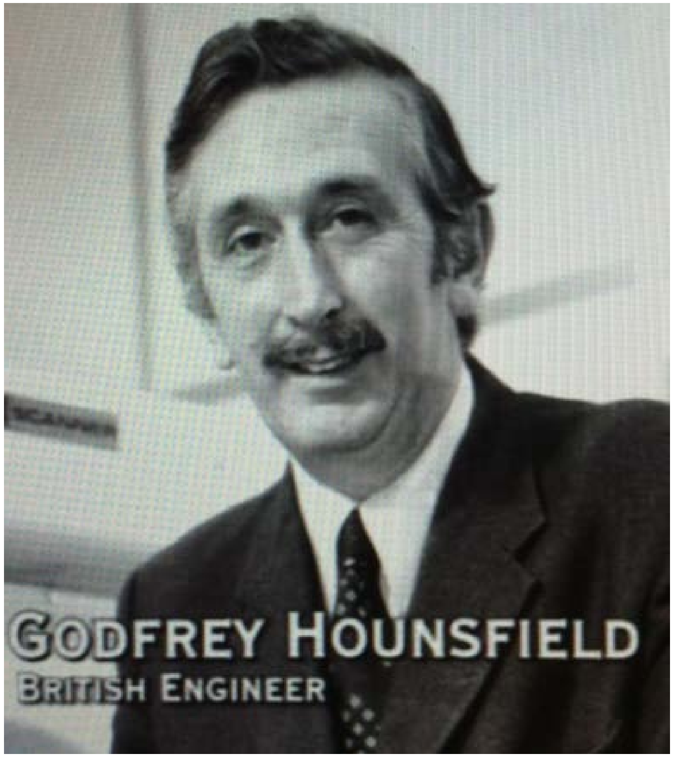

1979: Nobel Prize for Medicine

Maizlin, Zeev V. et a. J. Comp.Assisted Tomography 2012

CT BASIC PRINCIPLES

Rotating sample

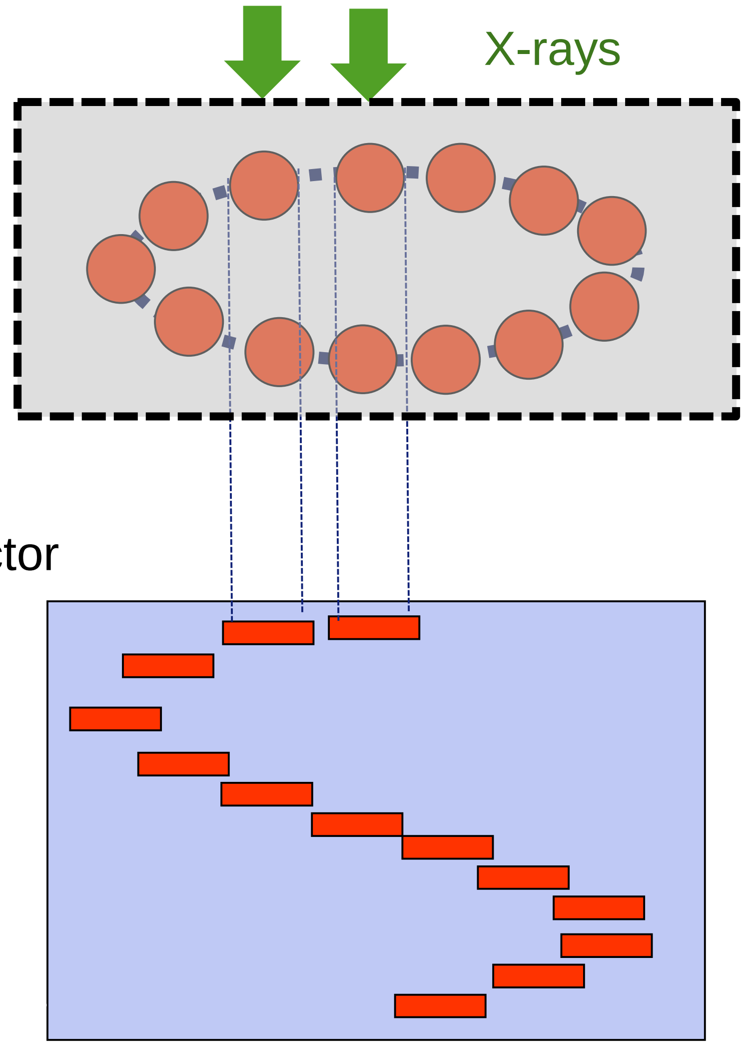

Detector

3D image

Computing (reconstruction algorithms)

Sinogram

0°

360°

STATE OF THE ART WHOLE BODY COMPUTED TOMOGRAPHY

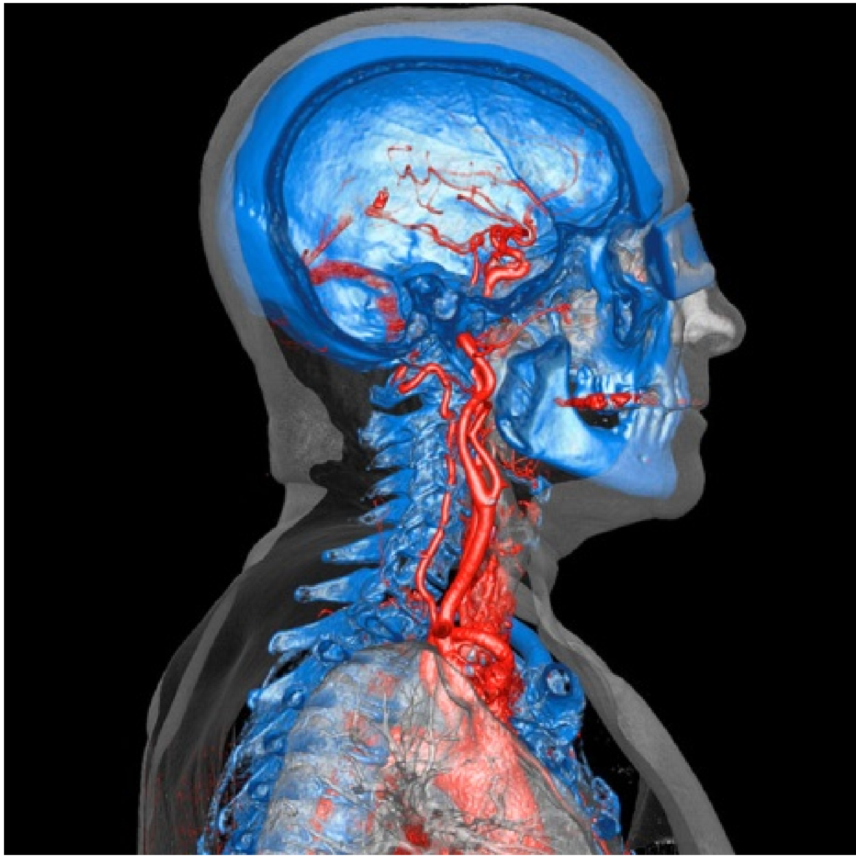

CHALLENGES IN CONVENTIONAL CT IMAGING

- **Limited spatial resolution: to 250 µm in clinics (dose) and ~3-10 µm in desktop scanners (large source size)**

- **Dose to the tissues -> increases with the square of the inverse of the pixel size**

  - **pediatric imaging (all organs)**
  - **prenatal imaging**
  - **radiosensitive organs (breast, thyroid, gonads, etc)**

- **Limited sensitivity for soft tissues --> limited diagnostic capability**

Phase contrast imaging:
an extremely powerful imaging technique

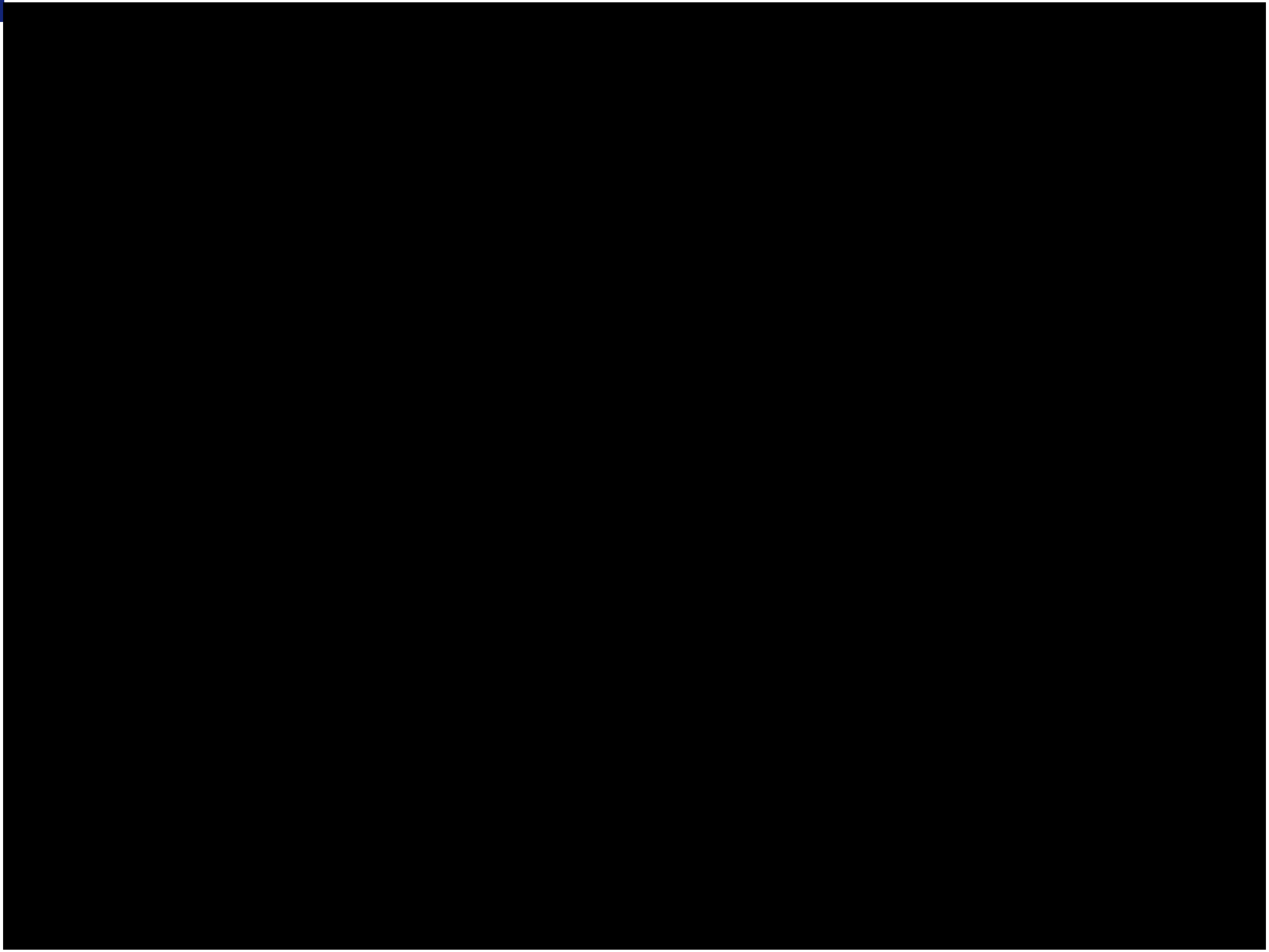

INTERFERENCE PHENOMENA ON A LAKE SURFACE

One source: circular waves

Two sources: interference

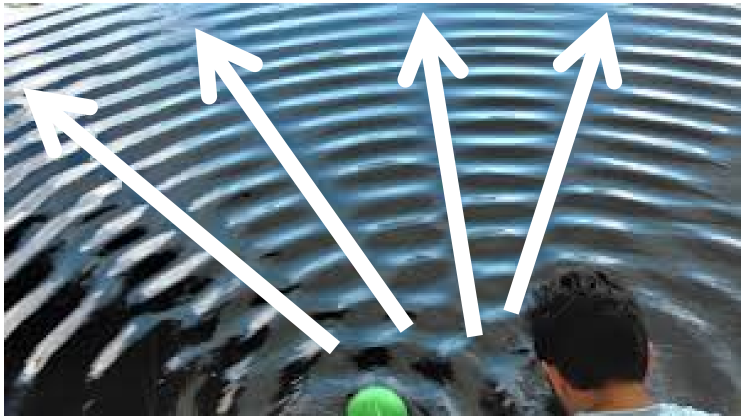

Interference peaks and valleys (no intensity)

IS LIGHT A WAVE?

YES and it shows all diffraction phenomena

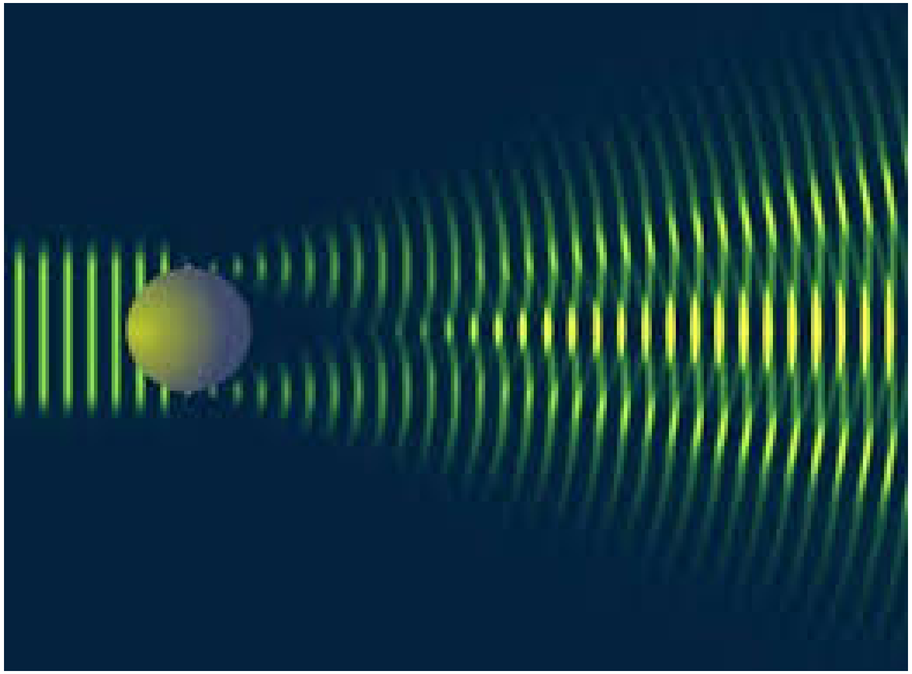

Green laser light on a ball: diffraction pattern
Side view

The same diffraction effects occur at X-ray wavelengths

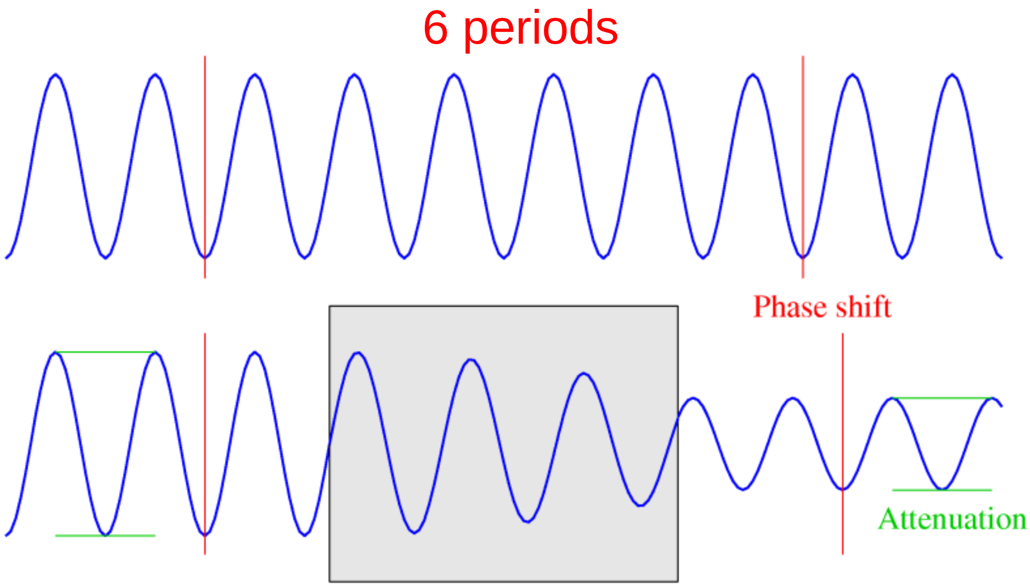

Free e.m. wave

The sample reduces wave amplitude and determines a phase shift

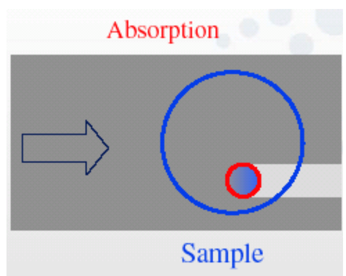

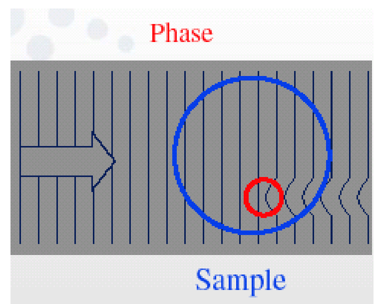

Sample transmission detection

⇩

Absorption coefficient mapping

Wave front modification

⇩

Phase contrast detection

$$n = 1 - \delta - i\beta$$

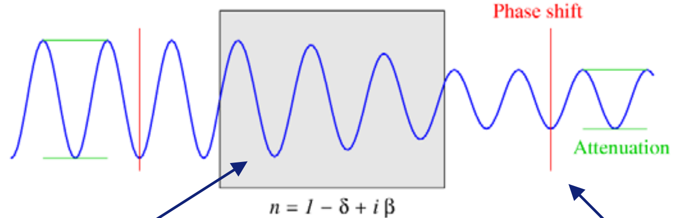

$$\beta = \frac{\lambda}{4\pi}\mu$$

Wave amplitude (absorption)

$$\delta = \lambda^2 \left(\frac{N_0}{A}\right) \rho_m r_0 \left(Z + f'\right)$$

Wave shift (refraction)

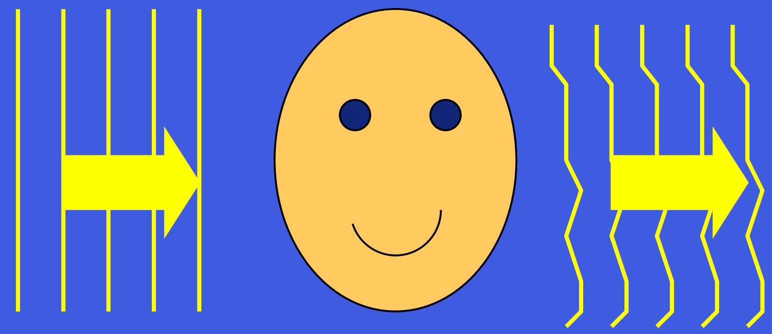

$A_{in}(x,y)$ $F(x,y)$ $A_o(x,y) = A_{in}(x,y)\, F(x,y)$

$F(x,y) = F_0(x,y)\, e^{i\varphi(x,y)}$

$$e^{-\frac{2\pi}{\lambda}\int \beta(x,y,z)\,dz}$$

Amplitude

$$\varphi(x,y) = \varphi_0 - \frac{2\pi}{\lambda}\int \delta(x,y,z)\,dz$$

Phase

THE DELTA/BETA GAIN!

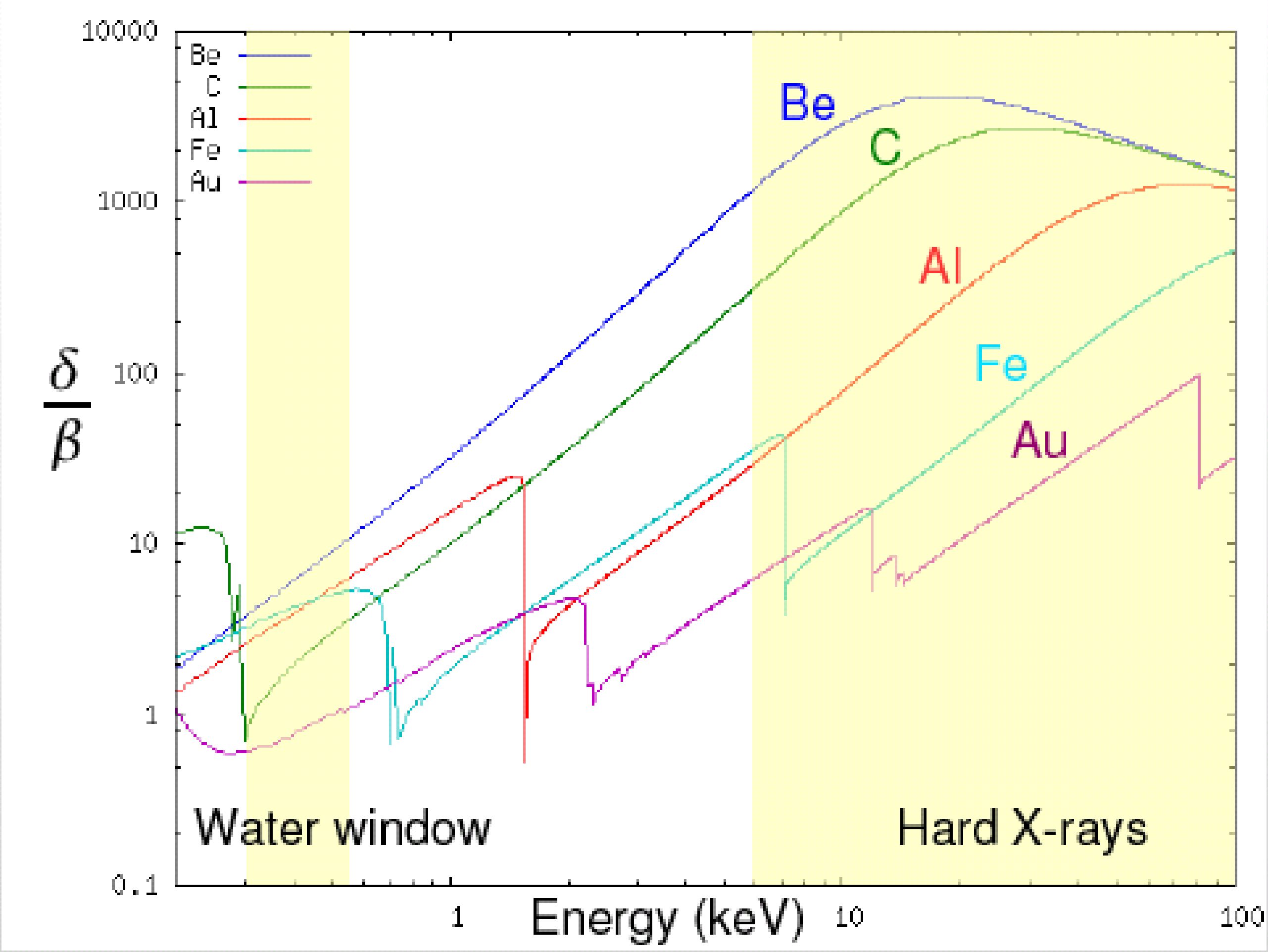

Gain of up to a few 1000 !

PHASE CONTRAST IMAGING: PROPAGATION BASED

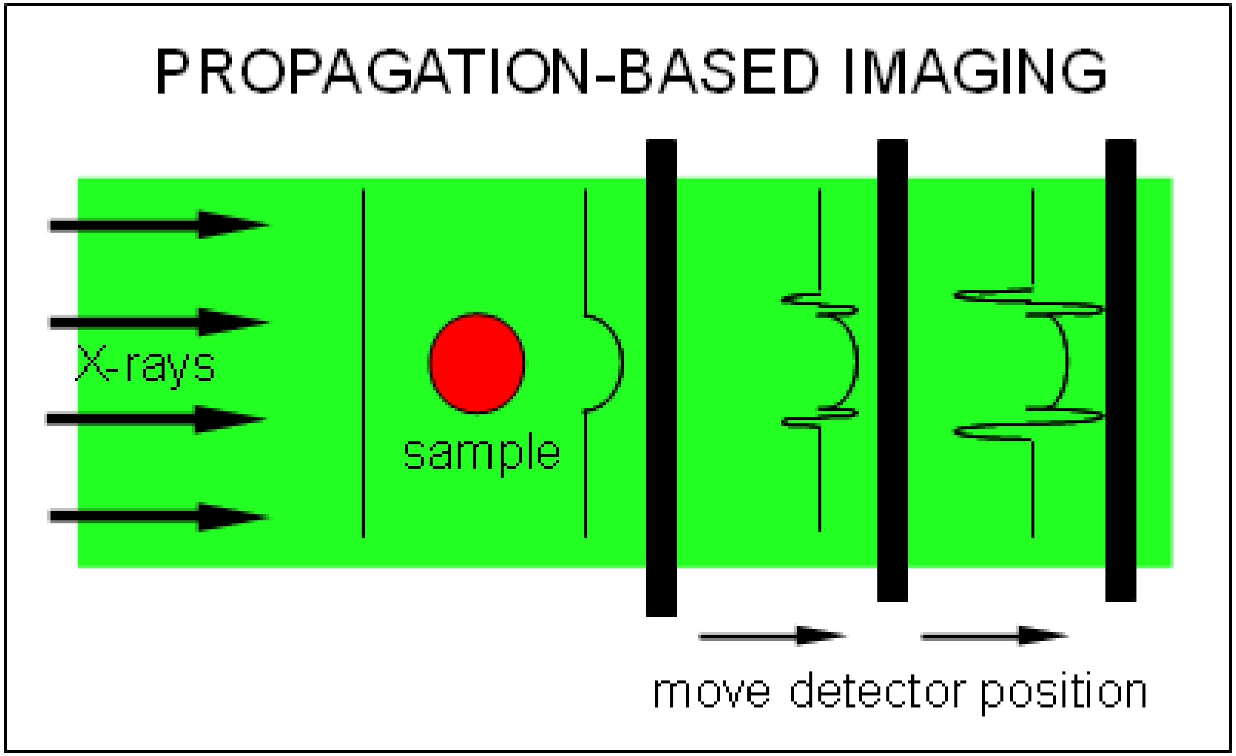

Intensity

$$I_D(\boldsymbol{x}) - I_0(\boldsymbol{x}) = -\frac{\lambda D}{2\pi} I_0(\boldsymbol{x}) \nabla[\nabla \varphi(\boldsymbol{x})]$$

Phase signal

(post-processing Paganin phase retrieval)

$$T(\boldsymbol{r}_\perp) = -\frac{1}{\mu}\log_e\left(F^{-1}\left\{\mu \frac{F\{M^2 I(M\boldsymbol{r}_\perp, z = R_2)\}/I^{in}}{\frac{R_2\delta|\boldsymbol{k}_\perp|^2}{M} + \mu}\right\}\right)$$

TECHNIQUES AVAILABLE FOR PHASE CONTRAST IMAGING

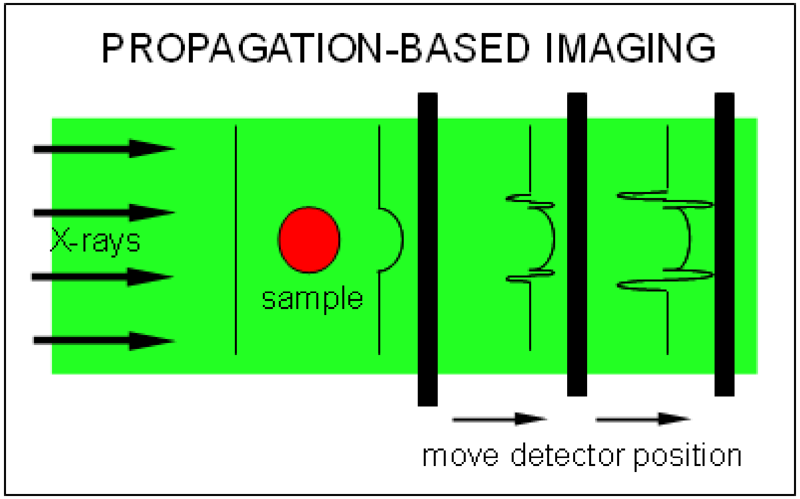

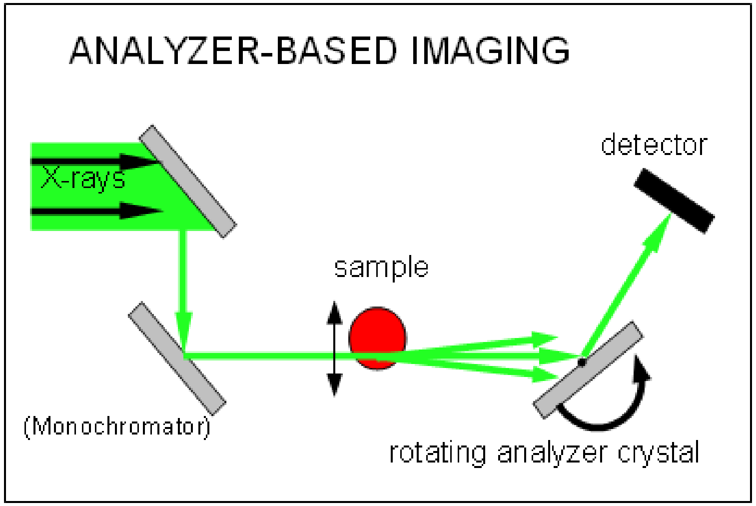

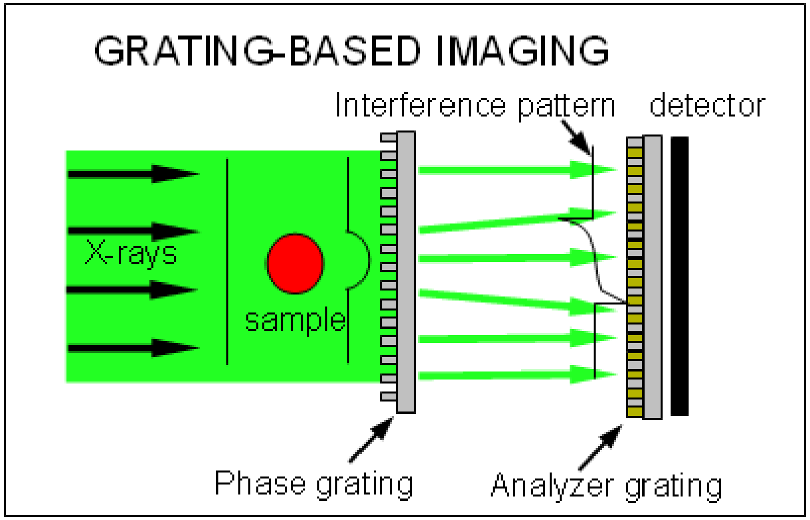

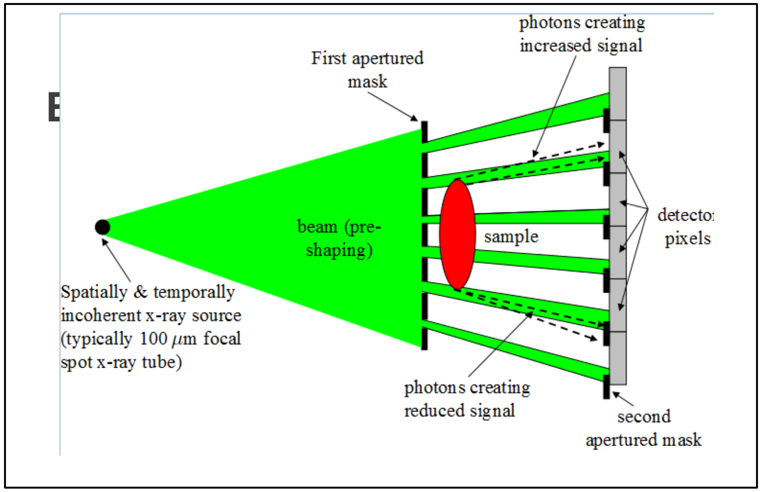

Optimal radiation is monochromatic collimated, and coherent X-rays, presently available only at synchrotron radiation sources

PHASE CONTRAST IMAGING APPLIED TO MEDICINE

Taking an X-ray image with early Crookes tube apparatus, 1896-1899.

Like for the X-ray discovery, medicine was immediately found as one of the most interesting final targets of phase contrast imaging

PHC IN THE 90IES: FROM NYLON WIRES TO FIRST MAMMOGRAPHY

Conventional radiography | **Phase contrast**

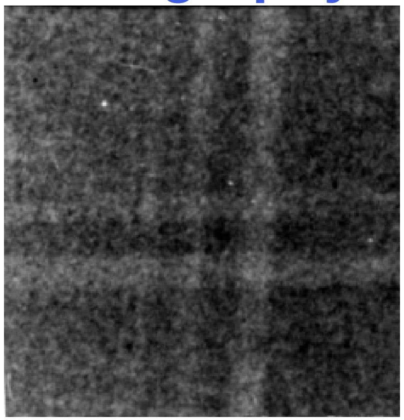

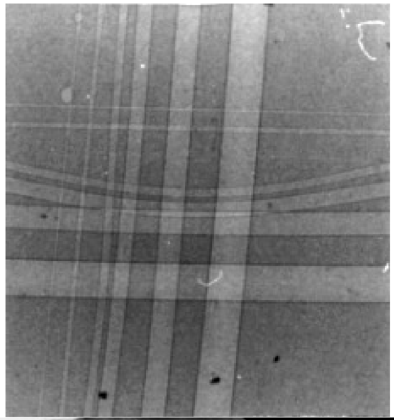

Images acquired at Elettra synchrotron, Trieste, 1997-1998

F.Arfelli, A. Bravin et al,
Physics in Medicine and Biology 43, 1998

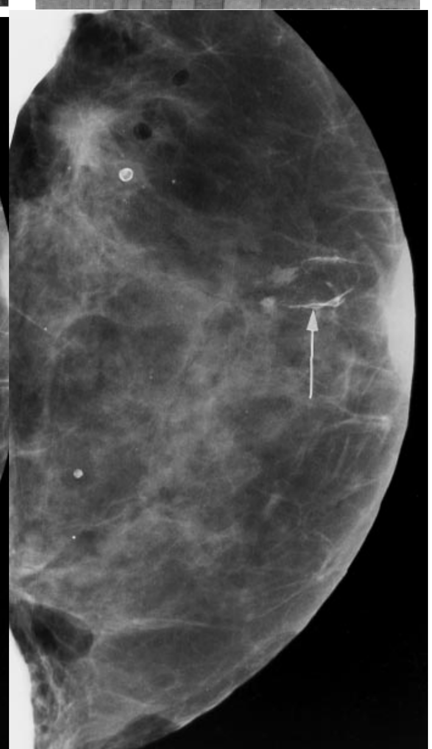

F. Arfelli, A. Bravin et al,
Radiology 215, 2000

LOW DOSE AND HIGH RESOLUTION HUMAN BREAST CT

Conventional

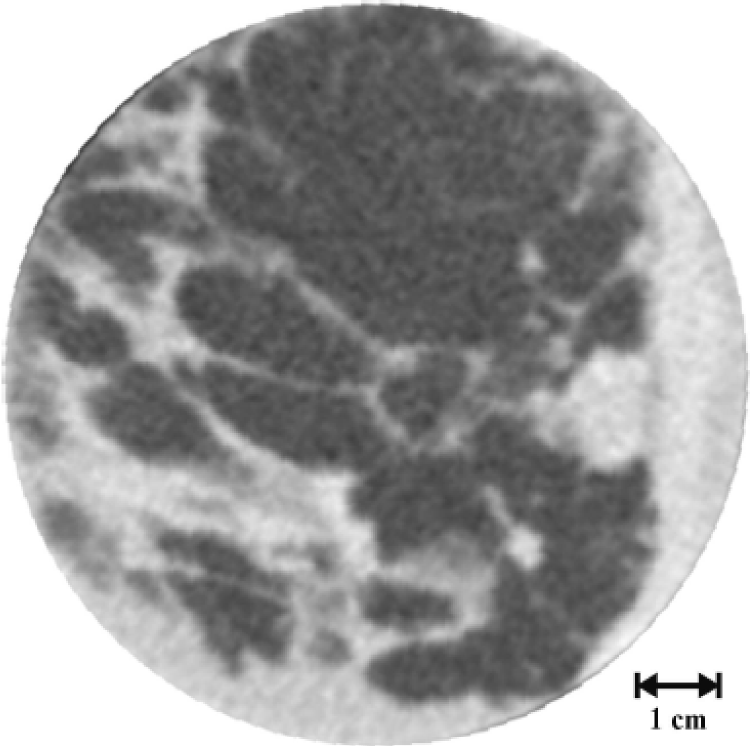

MGD=6.9 mGy

Phase contrast (ABI)

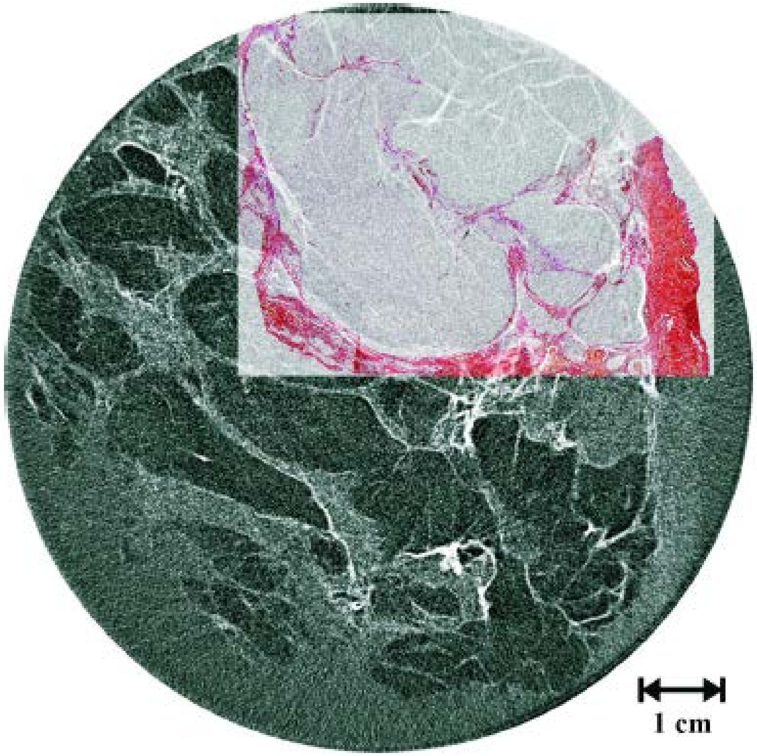

MGD=1.9 mGy

Keyriläinen et al. Radiology, 2008

OSTEOARTHRITIC AND NORMAL HUMAN PATELLA CARTILAGE

26 keV
Si (333)
8 µm pixel size

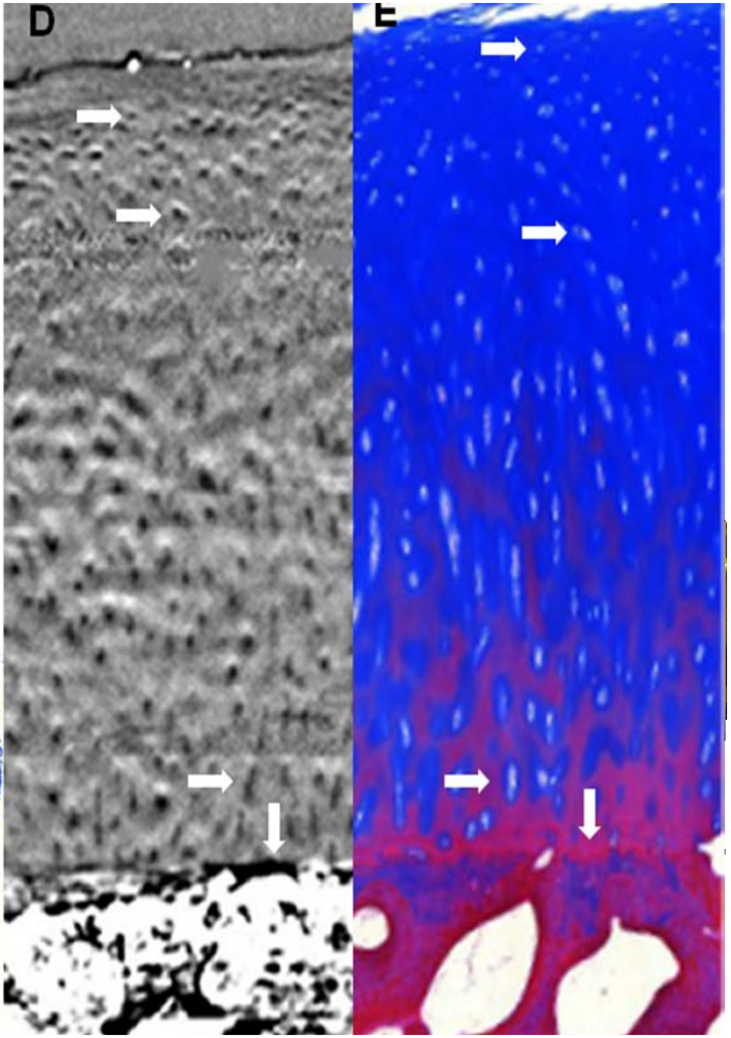

Correlation with histology

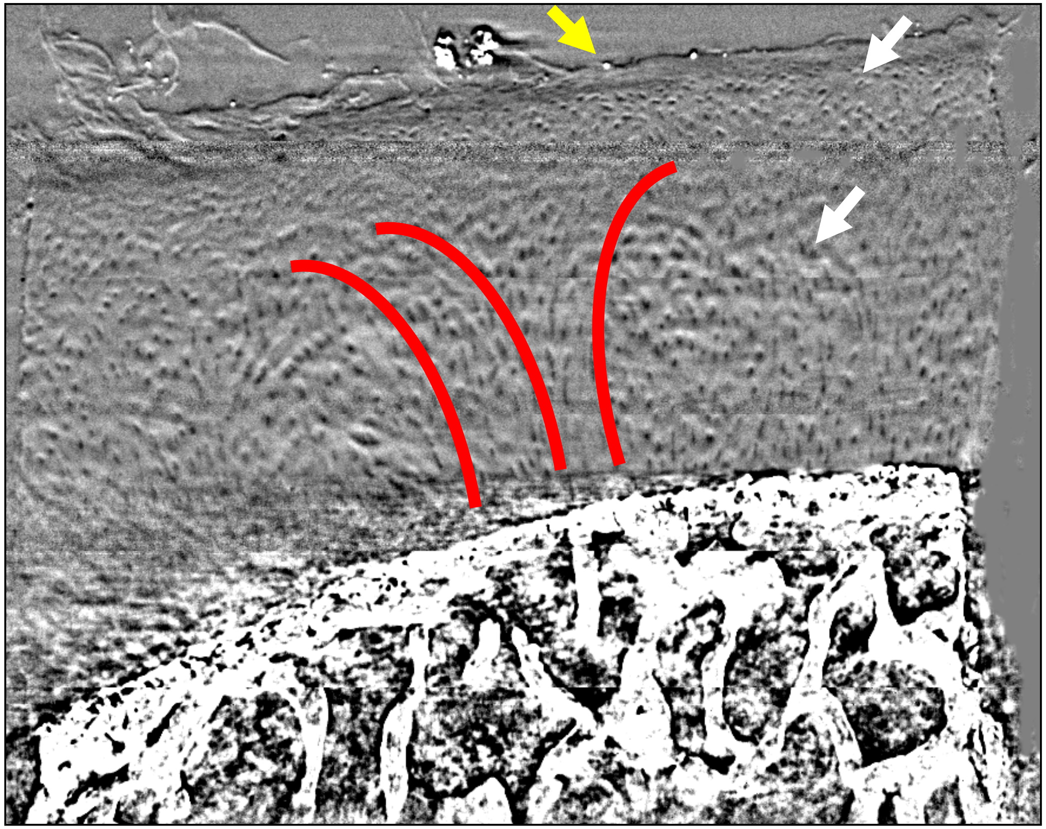

Coan et al. Inv. Rad. 2010 Jul;45(7):437

CT OF FULL HUMAN KNEES (POST MORTEM)

Conventional CT

MRI

PCI- CT

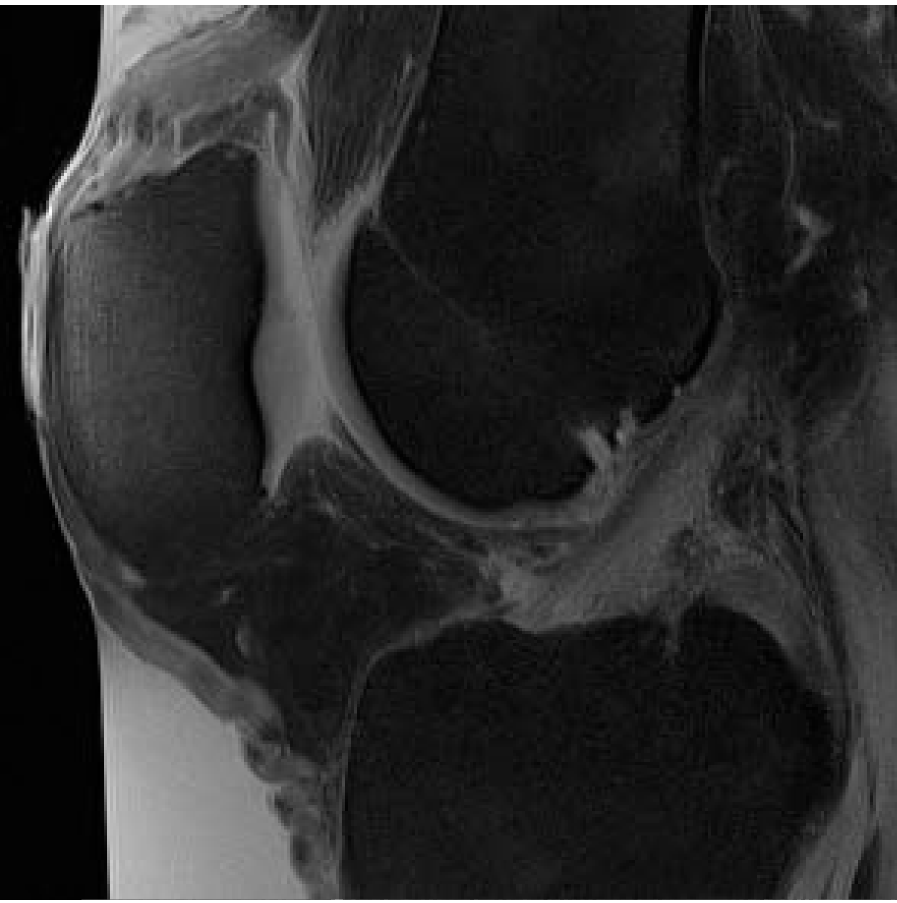

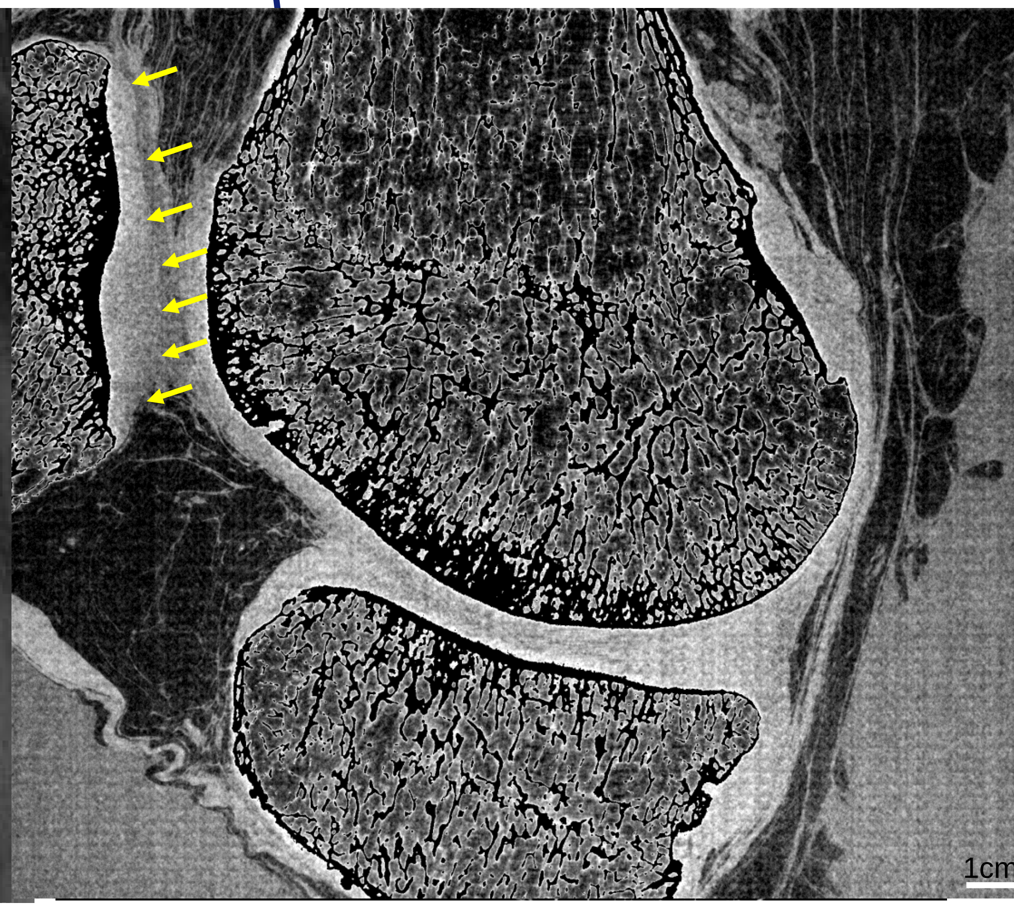

bone image

soft tissue image

Horng et al. Inv. Rad. 2014 Sep;49(9):627-34

HIGH-RESOLUTION PHASE-CONTRAST CT OF FULL HUMAN KNEES

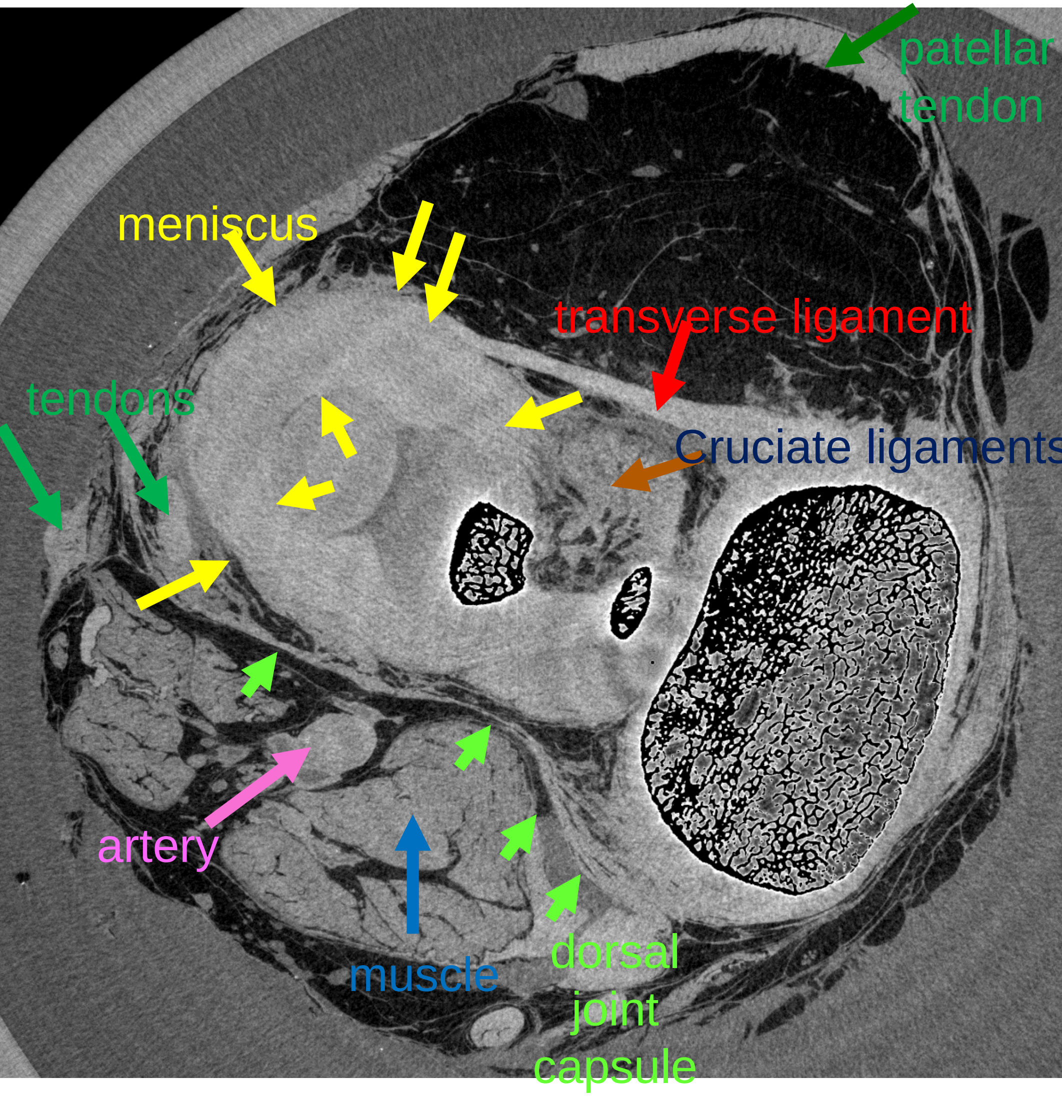

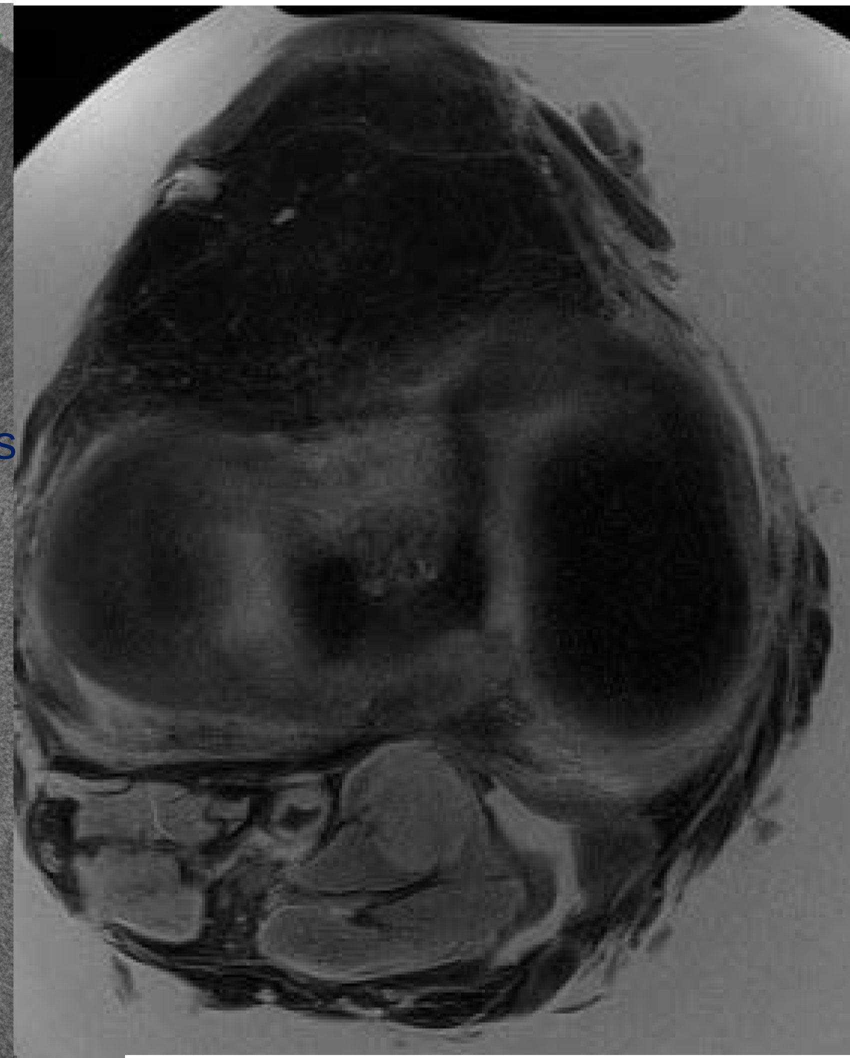

Horng et al. Invest. Radiol. 2014

Applications to neurosciences

(since ~2000)

HIGH RESOLUTION PCI-CT ON HEALTHY AND PATHOLOGICAL RAT BRAIN

Assessing the microscopic effects of radiation therapy on brain tumors in brains (microvasculature)

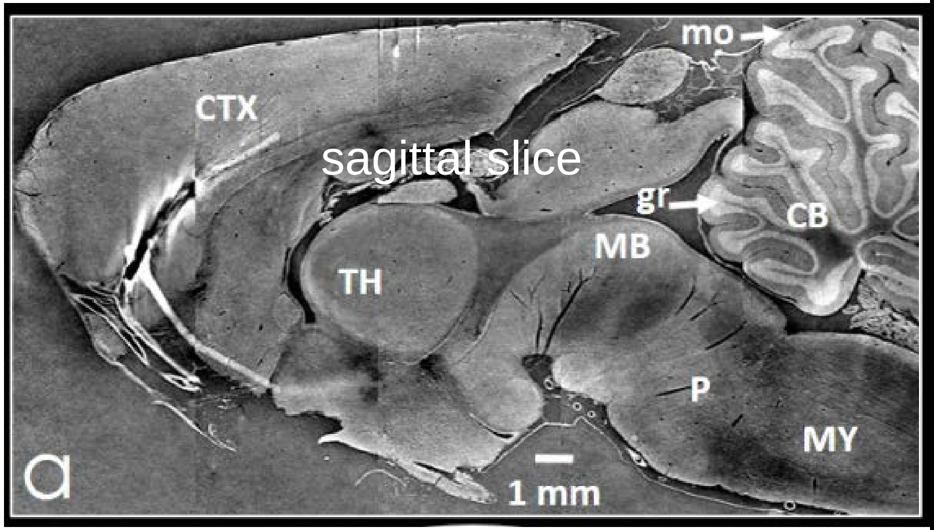

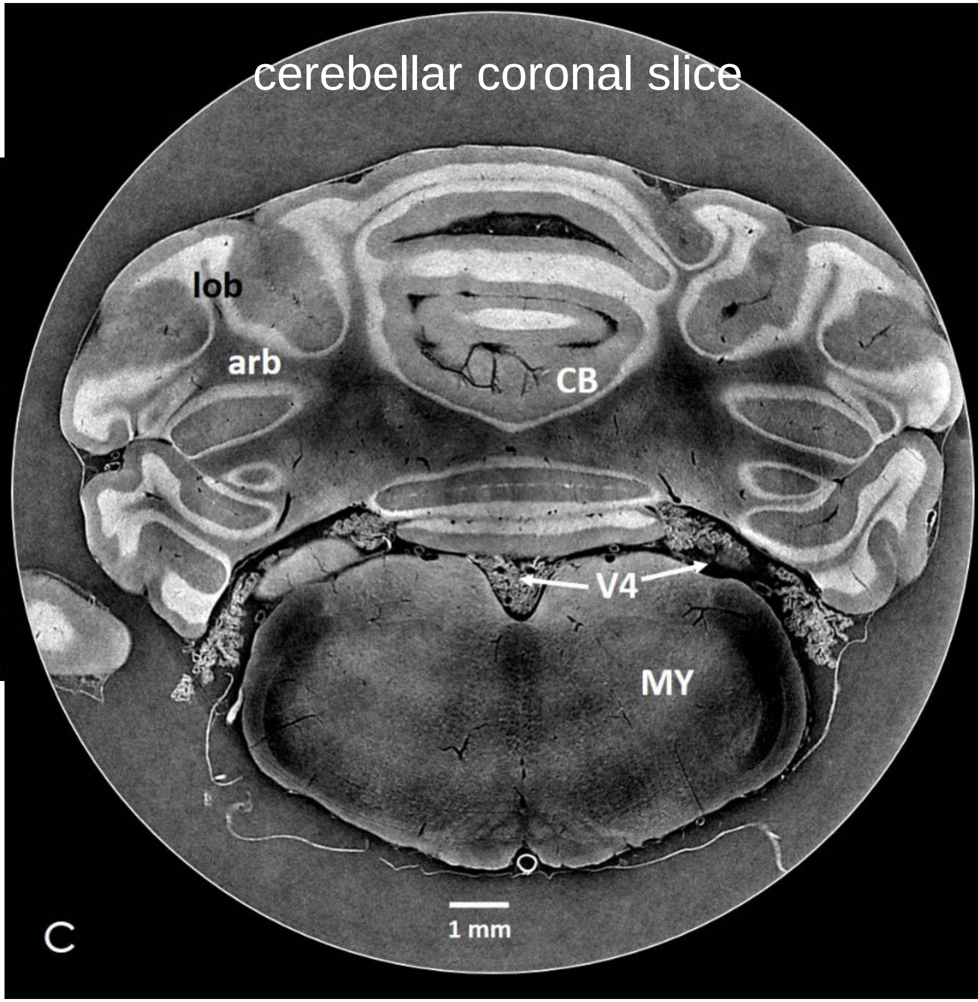

Pixel size: 7.9 micron
PCI technique
Paganin's phase retrieval

Barbone et al., Int J Radiation Oncol Biol Phys, Vol. 101, No. 4, pp. 965-984, 2018

HIGH RESOLUTION PCI-CT ON HEALTHY RAT BRAIN

Dorsal hippocampus, Hammon's Horn and Dentate Gyrus

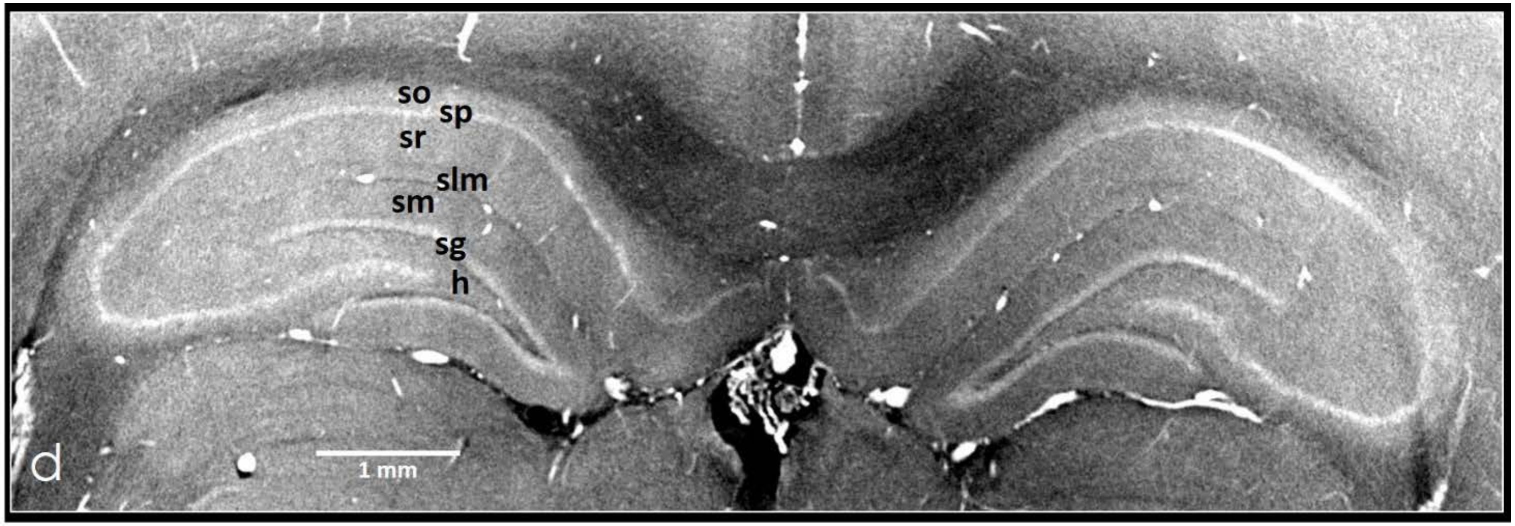

third (V3) and lateral ventricles (VL)

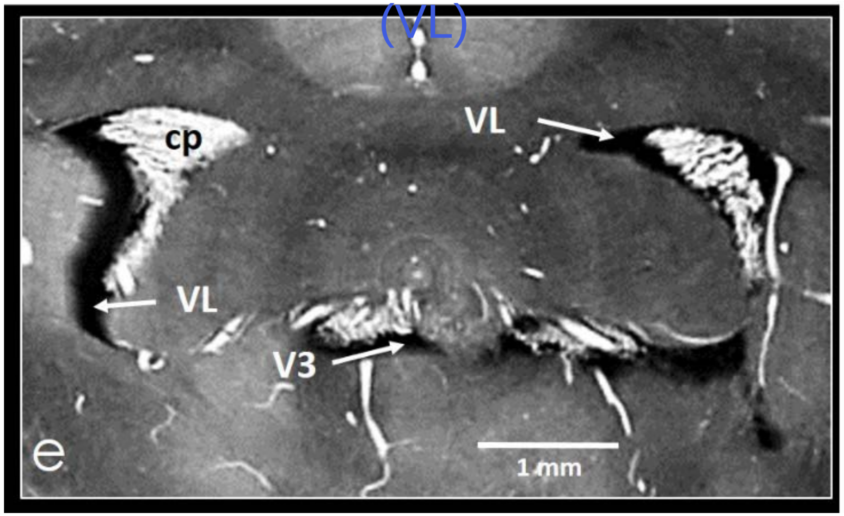

the striated architecture of the caudate-putamen

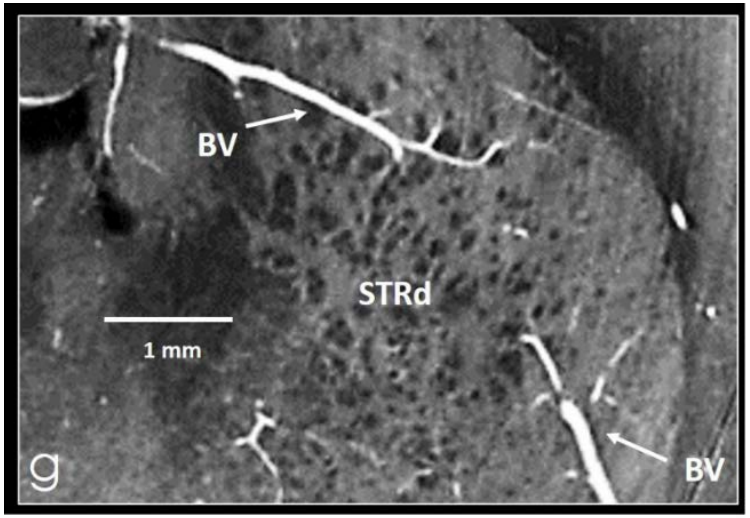

Barbone et al., Int J Radiation Oncol Biol Phys, Vol. 101, No. 4, pp. 965-984, 2018

PHASE CONTRAST MICRO-CT VS MRI

Rat hippocampus

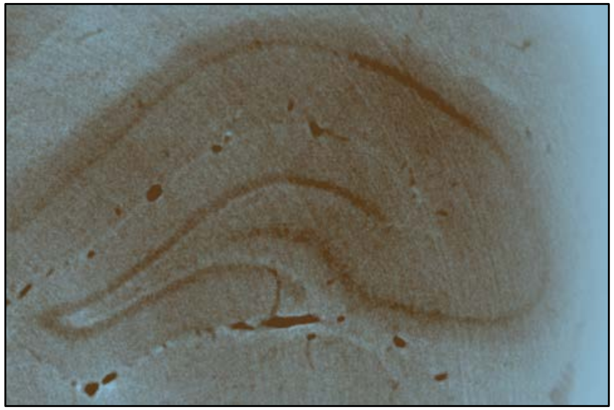

Phase contrast imaging

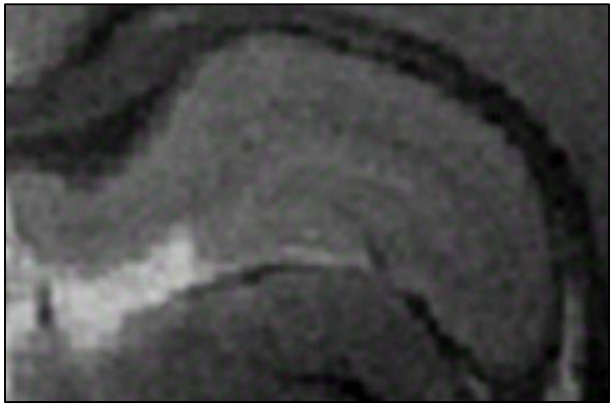

7T MRI

Histology

Pixel size: 7.9 micron
PCI technique
Paganin’s phase retrieval

 Barbone et al., Int J Radiation Oncol Biol Phys, Vol. 101, No. 4, pp. 965-984, 2018

HIGH RESOLUTION PCI-CT ON HEALTHY RAT BRAIN

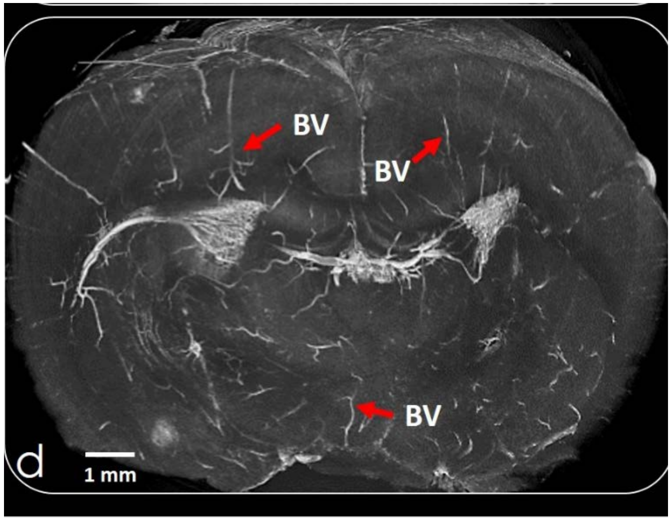

d. microscopic (> 16 µm-thick) superficial and internal blood vessels

e. brain intra-cortical vessel-tree 3D segmentation

f. zoom-in of densely-packed deep micro-vasculature

NO CONTRAST AGENT USED

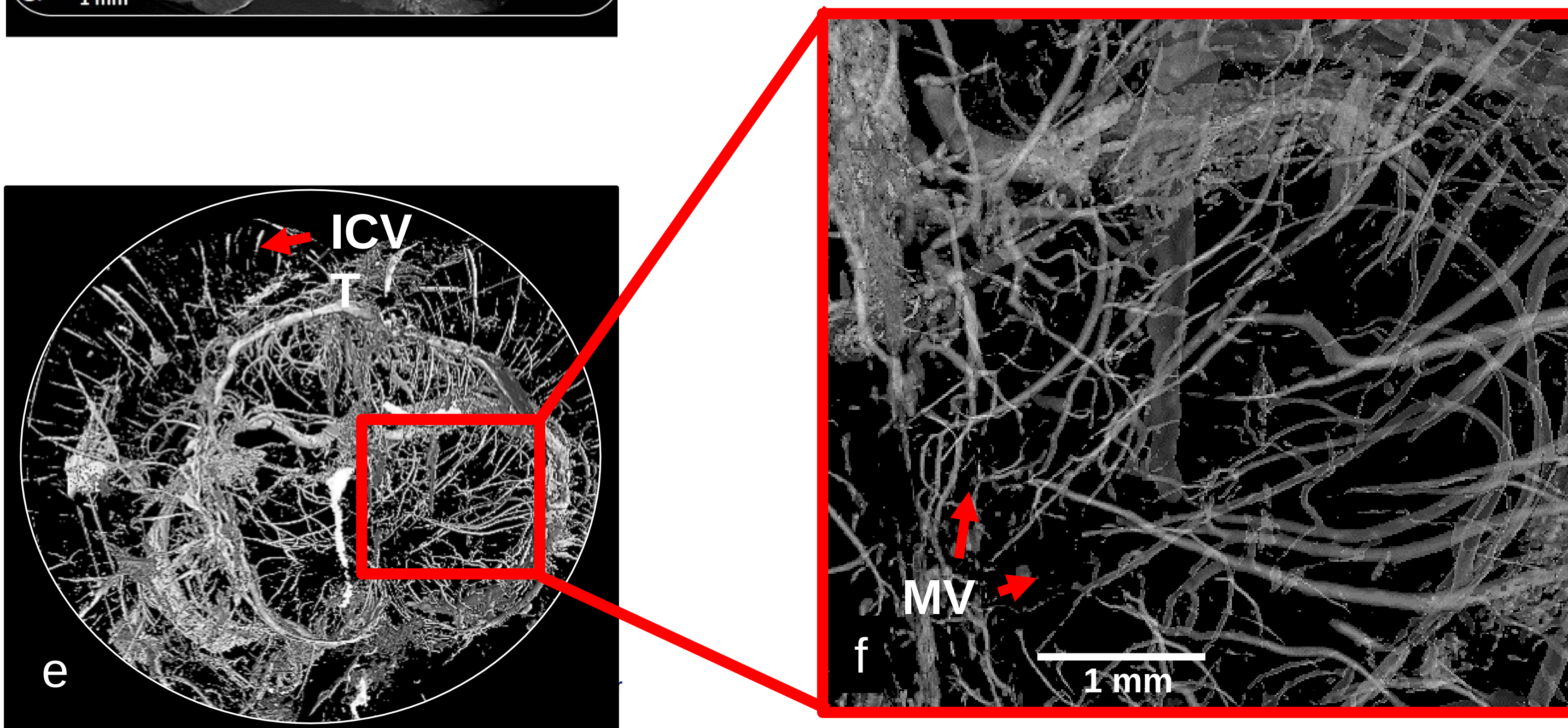

HIGH RESOLUTION PCI-CT ON TUMOR BEARING RAT BRAIN

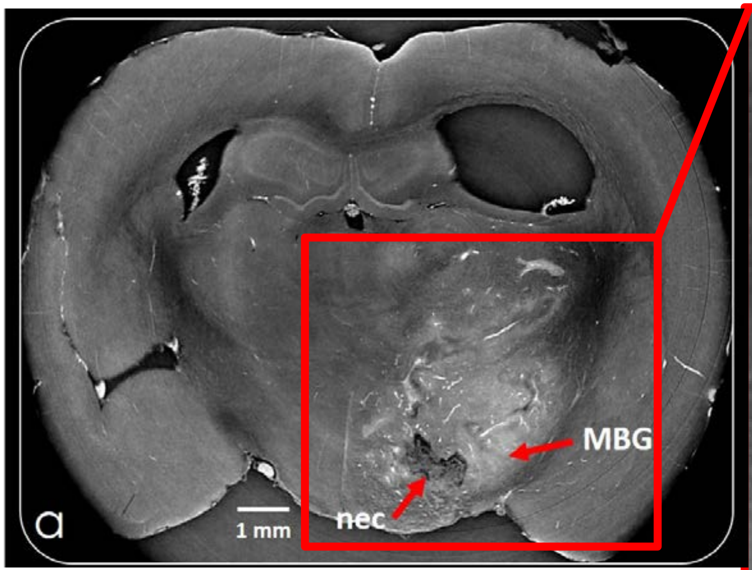

a. coronal 9L glioblastoma in the thalamus

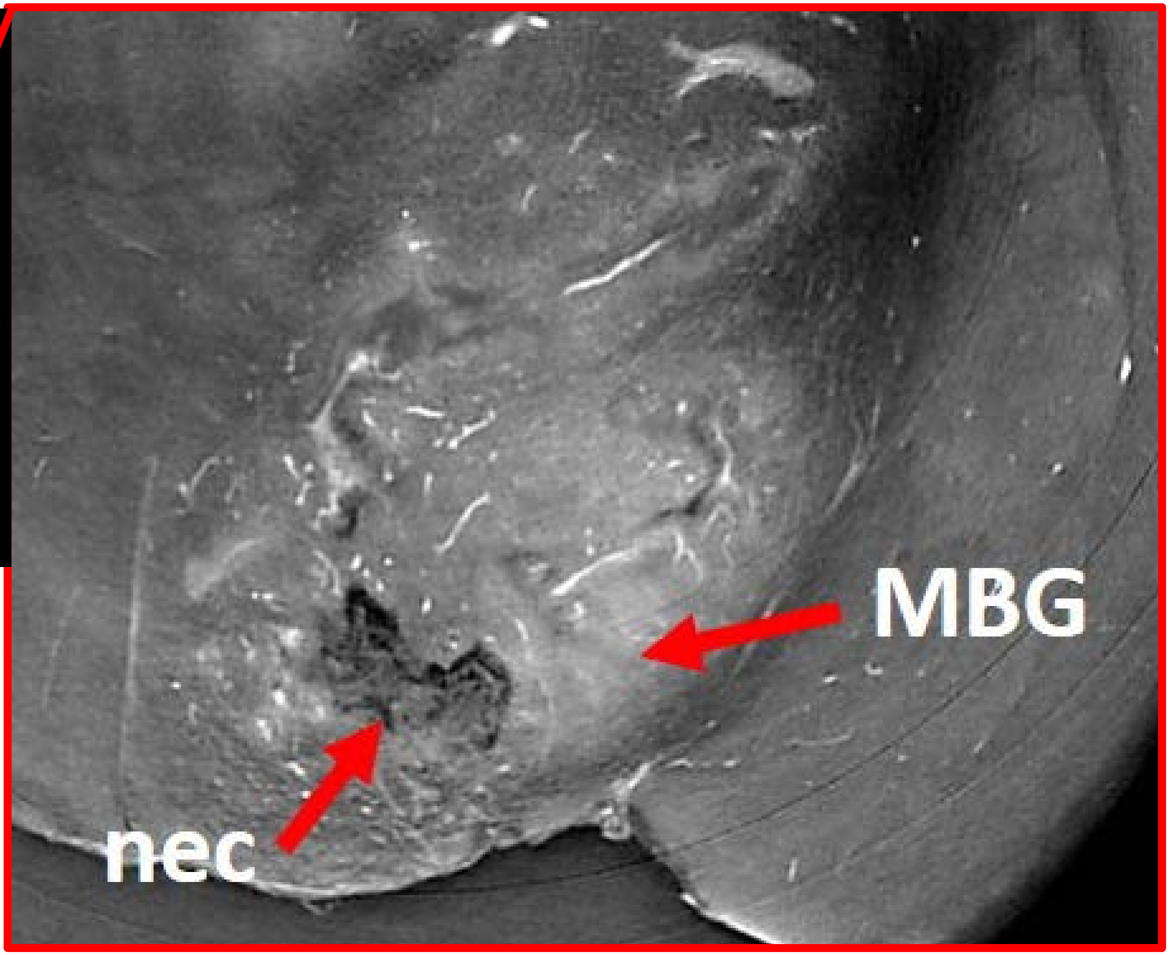

b. GBM tissue infiltration : island-like and tentacular cancer regions invading healthy tissue

Pixel size: 7.9 micron
PCI technique
Paganin's phase retrieval

 Barbone et al., Int J Radiation Oncol Biol Phys, Vol. 101, No. 4, pp. 965-984, 2018

Simultaneous submicrometric 3D imaging of the micro-vascular network and the neuronal system in a mouse spinal cord

Michela Fratini[1,2], Inna Bukreeva[3], Gaetano Campi[4], Francesco Brun[5,6], Giuliana Tromba[6], Peter Modregger[7], Domenico Bucci[8], Giuseppe Battaglia[8], Raffaele Spanò[9], Maddalena Mastrogiacomo[9], Herwig Requardt[10], Federico Giove[1,11], Alberto Bravin[10] & Alessia Cedola[3]

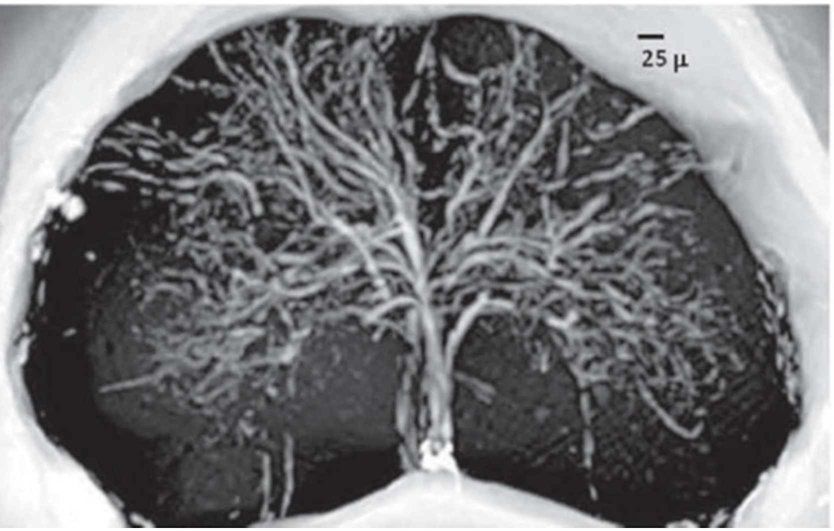

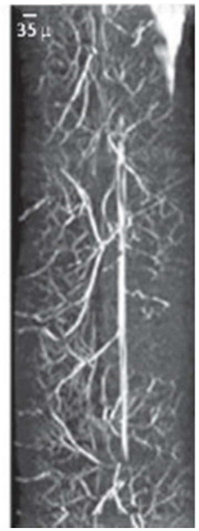

ID17, ESRF
Tomcat, PSI

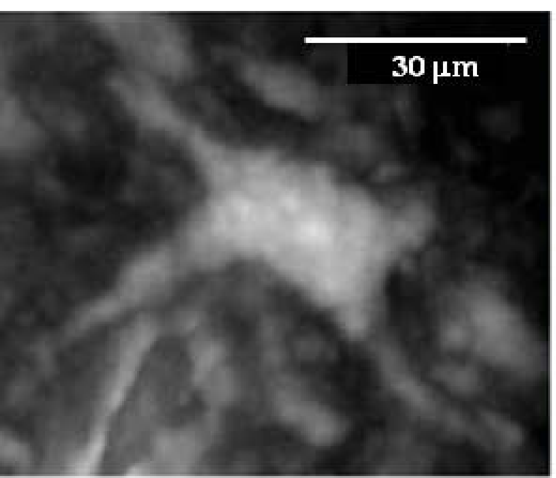

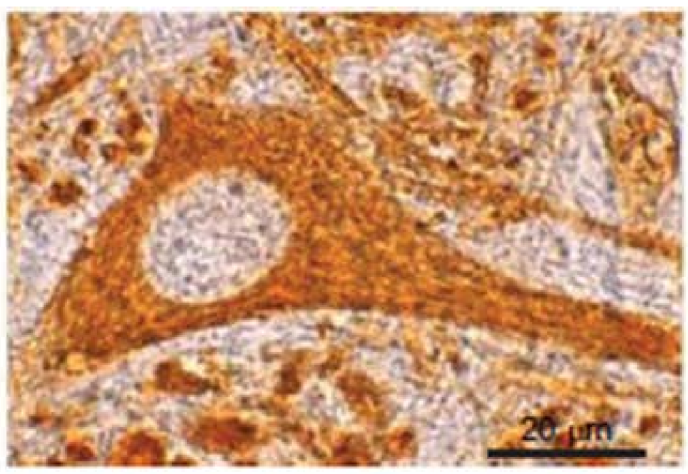

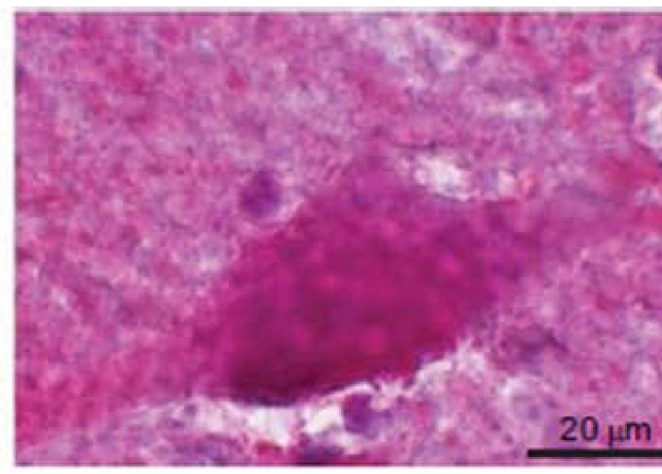

Multiple Sclerosis is an autoimmune disease leading to demyelination, axonal damage and neuronal loss.

Alterations in **vasculature** are a central component of the demyelinating diseases

Study made on experimental **autoimmune encephalomyelitis mouse** model

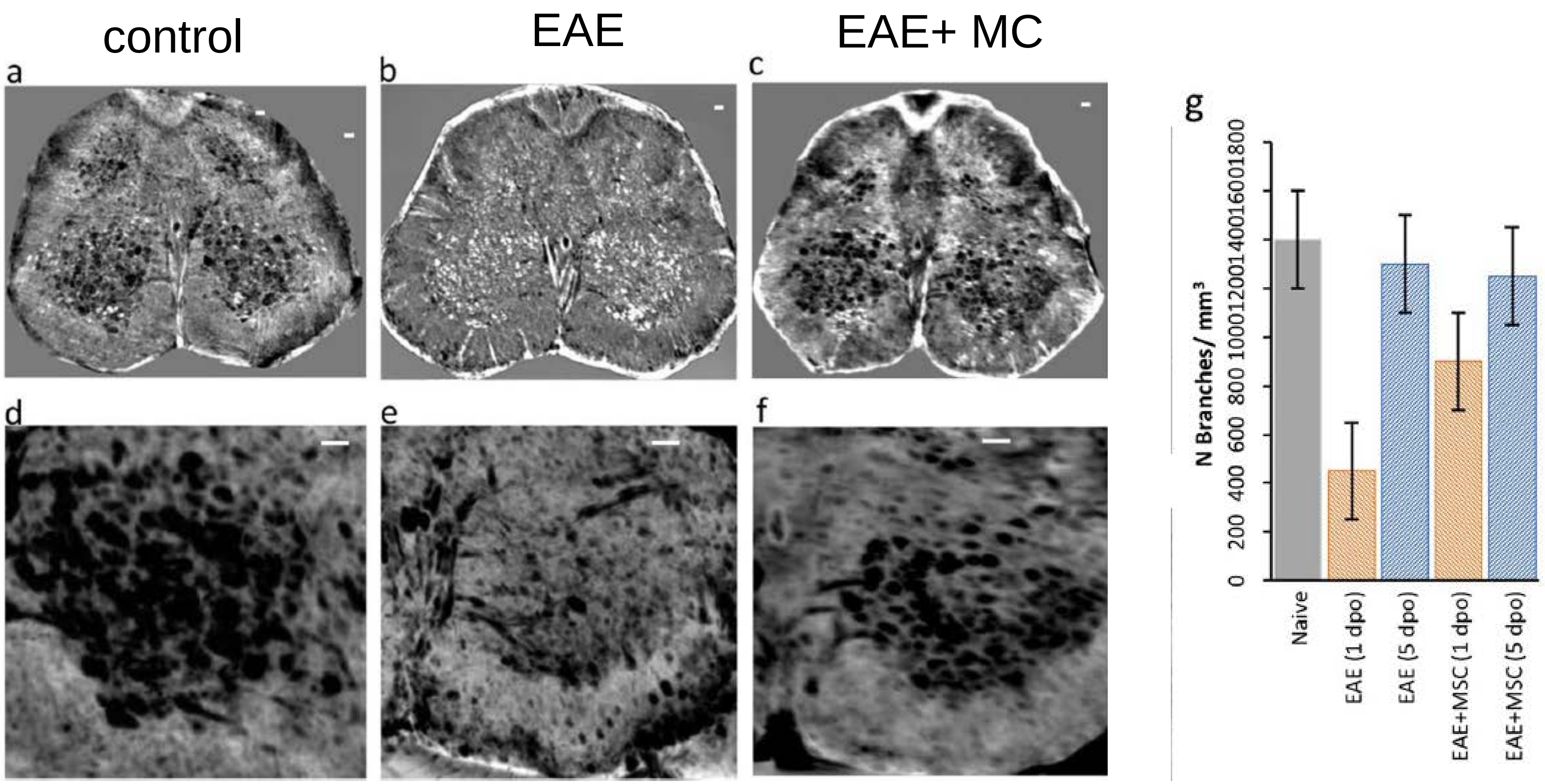

Lumbar spinal cord. Pixel size: 3.1 micron, bar: 20 micron

A. Cedola, A. Bravin et al. Scientific Reports Jul 19;7(1):5890 (2017)

EAE untreated

EAE+ MC

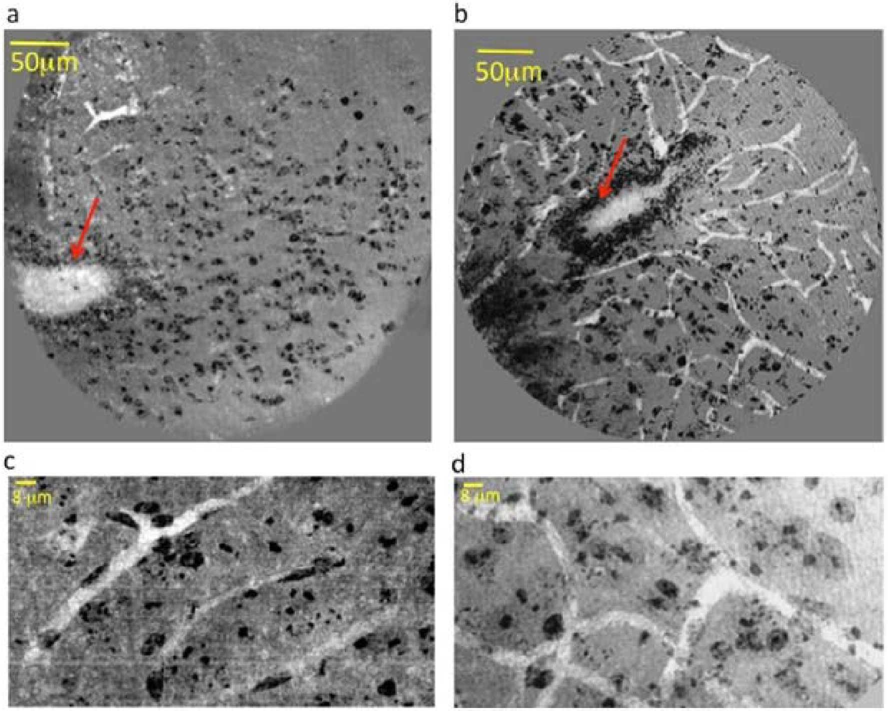

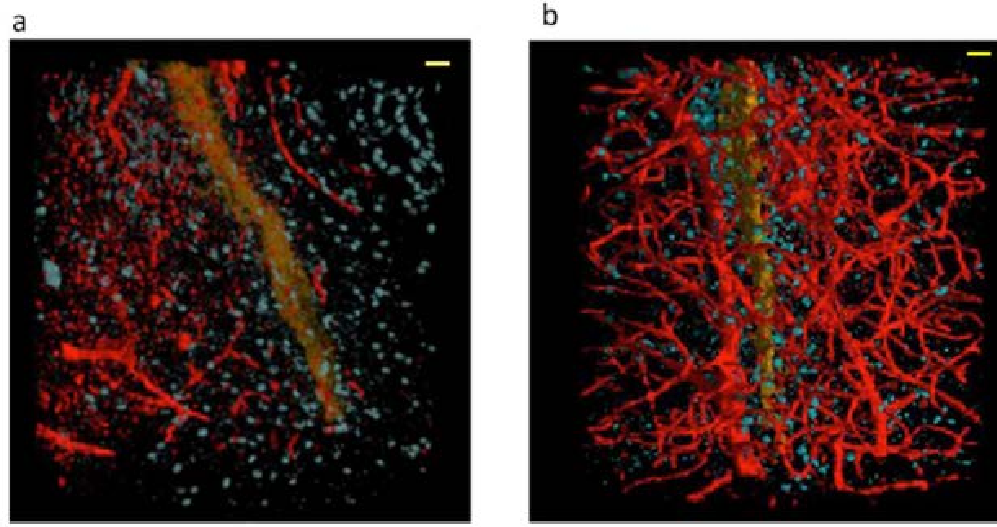

Scale bar: 8 μm

Animals sacrificed 5 days from onset. Pixel size: 130 nm

Decrease in vessel density at disease onset as compared to healthy mice, which was not observed in EAE-affected mice treated with MSC.

A. Cedola, A. Bravin et al. Scientific Reports Jul 19;7(1):5890 (2017)

Mouse spinal cord, post-mortem
Voxel: 3.5^2 μm^2 x 1 mm

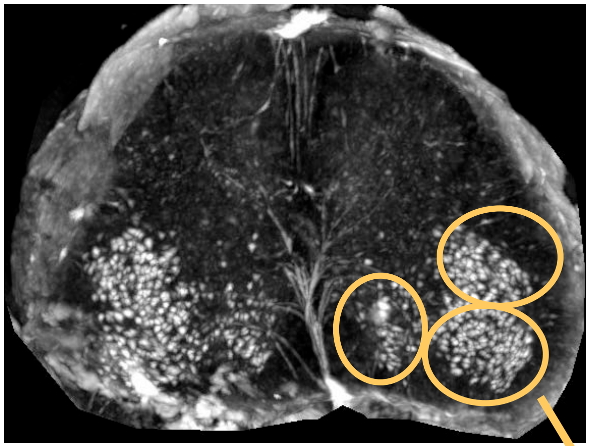

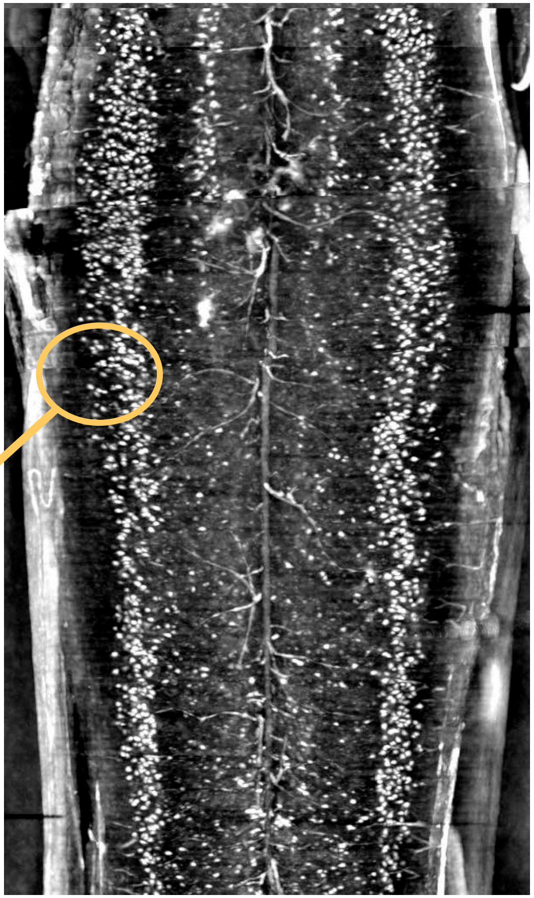

Motor neuron nuclei in axial and coronal view

G. Begani Provinciali, F. Palermo, M. Fratini, I. Bukreeva, A. Cedola, et al, CNR-Nanotec, unpublished

MONKEY EYE

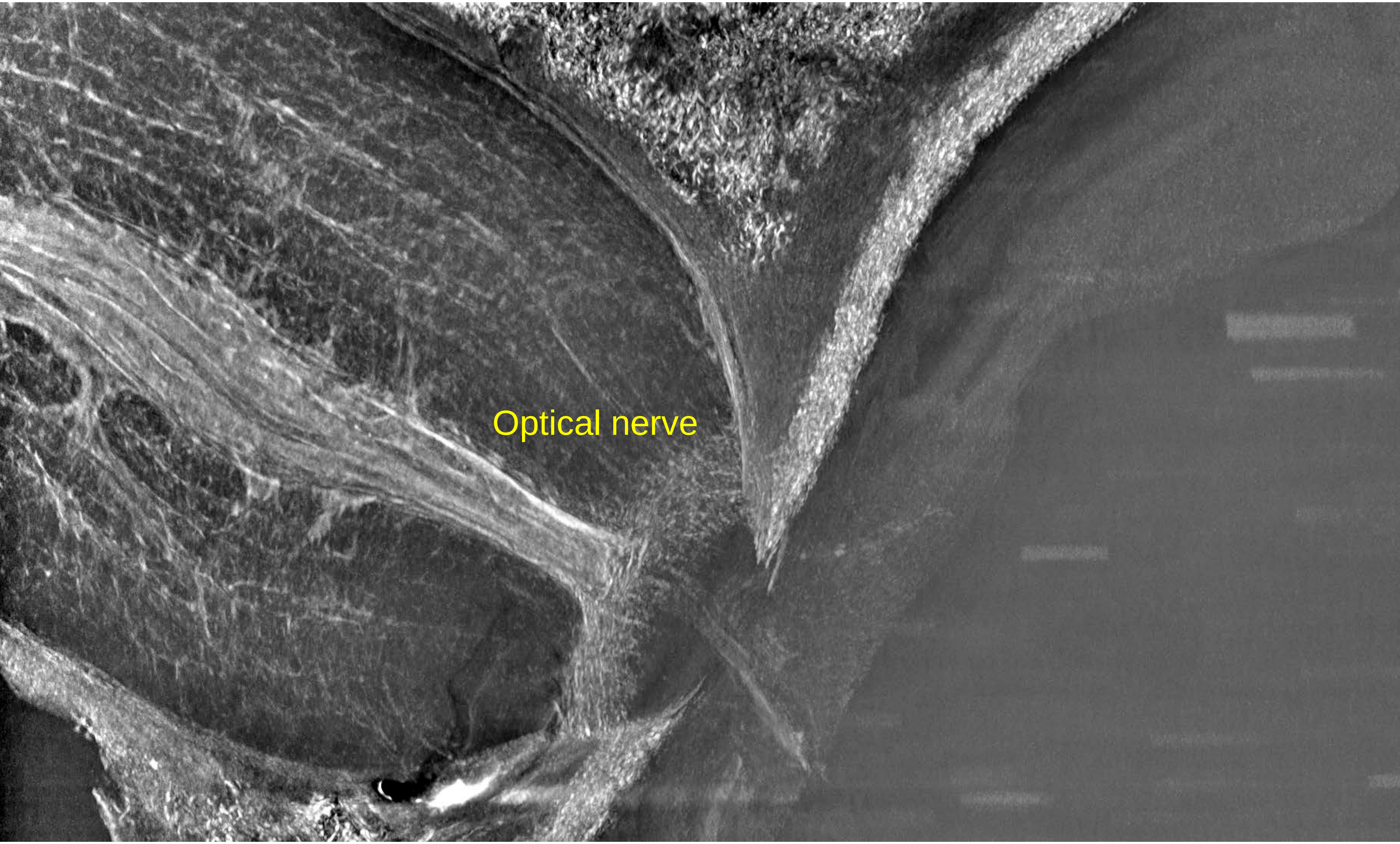

A. Mittone, et al. Physica Medica 51 (2018) 7–12

WHAT IS A SYNCHROTRON?

“A very large microscope to see deep inside matter”

- A source of X-rays produced by relativistic electrons of special characteristics:

- Extremely intense: the most intense on earth

- Highly collimated

- Brilliant

- Tunable in energy

A synchrotron in a nutshell…

Conventional source:

- Incoherent (and polychromatic) light
- Cone beam geometry
- Limited photon flux

Synchrotron source:

- Coherent (and monochromatic) light
- (Nearly) parallel beam geometry
- High photon flux ➡ very fast CT

SYNCHROTRON RADIATION FOR MEDICAL APPLICATIONS

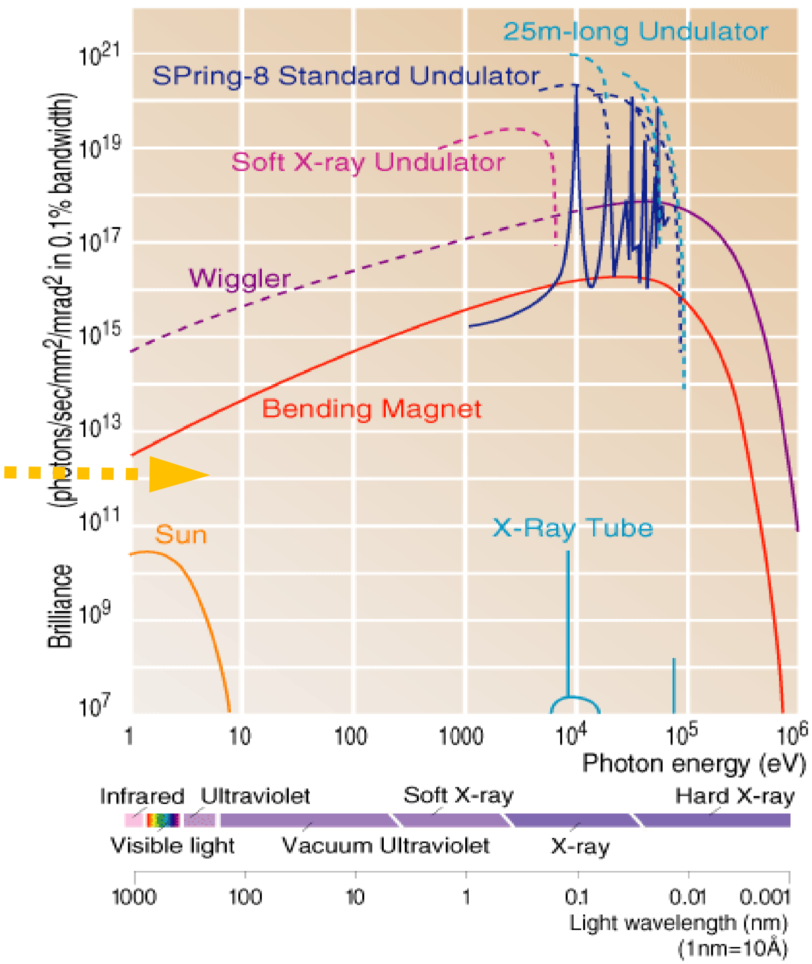

Why is SR interesting for imaging?

- ~10^6X more intense than medical X-ray generators or LINACS
- tunable monochromatic energy
- parallel beam
- micrometric spatial resolution

A SYNCHROTRON IN 30”

Credits to: YouTube “Synchrotron technology Diamond Light Source”.
“Europe's premier X-ray source”

WALKING NEXT TO THE ESRF ELECTRON STORAGE RING

SYNCHROTRONS IN THE WORLD

3 larger facilities

5 with dedicated medical beamlines

THE ESRF AND THE ID17 MEDICAL BEAMLINE

The ESRF today – a consortium of 22 Countries

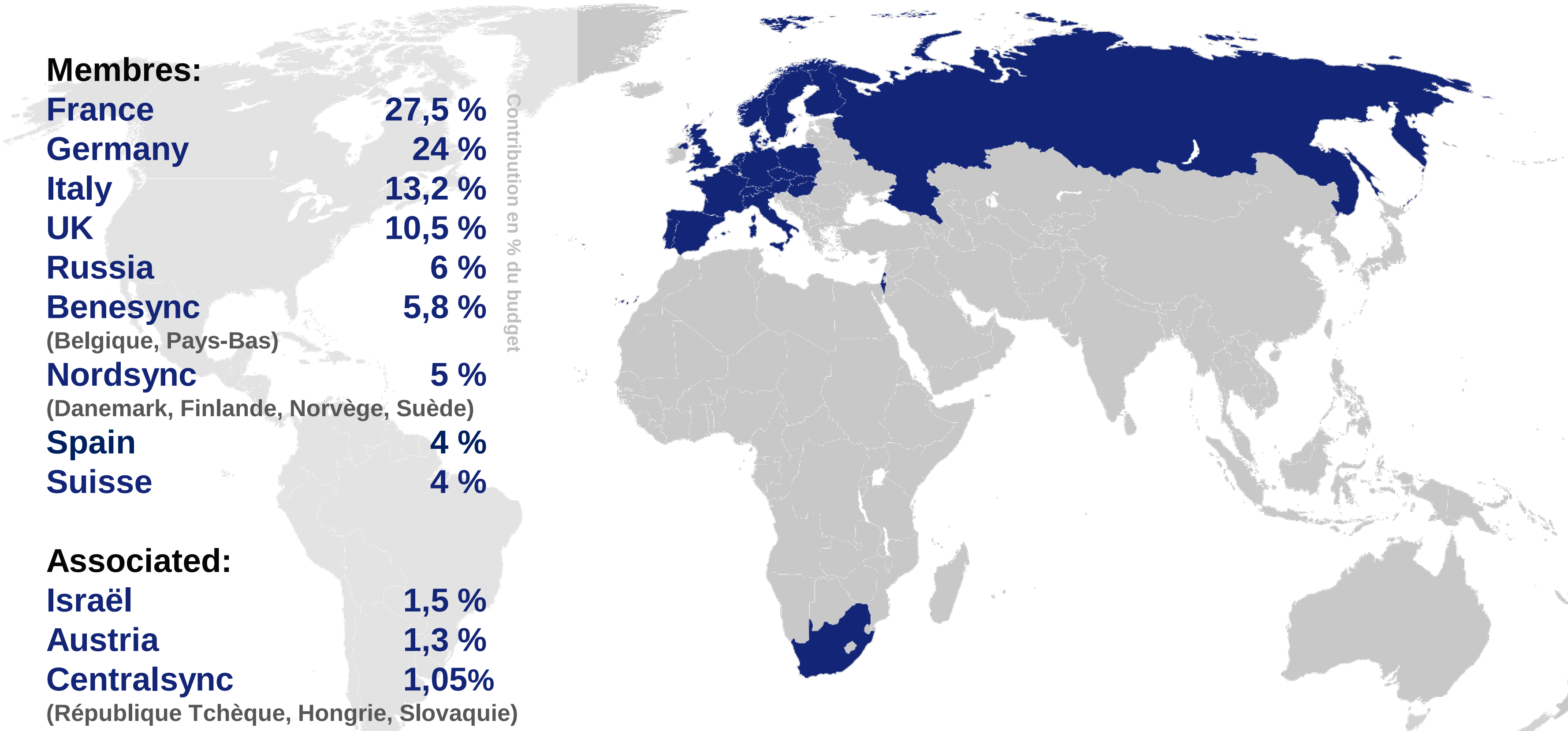

Membres:

France	27,5 %
Germany	24 %
Italy	13,2 %
UK	10,5 %
Russia	6 %
Benesync (Belgique, Pays-Bas)	5,8 %
Nordsync (Danemark, Finlande, Norvège, Suède)	5 %
Spain	4 %
Suisse	4 %

Associated:

Israël	1,5 %
Austria	1,3 %
Centralsync (République Tchèque, Hongrie, Slovaquie)	1,05%
Polonie	1 %
Portugal	1 %
India	0,66%
South Africa	0,3 %

Contribution en % du budget

Annual Budget: 100 millions euro
Personnel : 630 employees, from 40 different countries

Monochromatic beam hutch:
Imaging &
Stereotactic Synchrotron Radiation Therapy

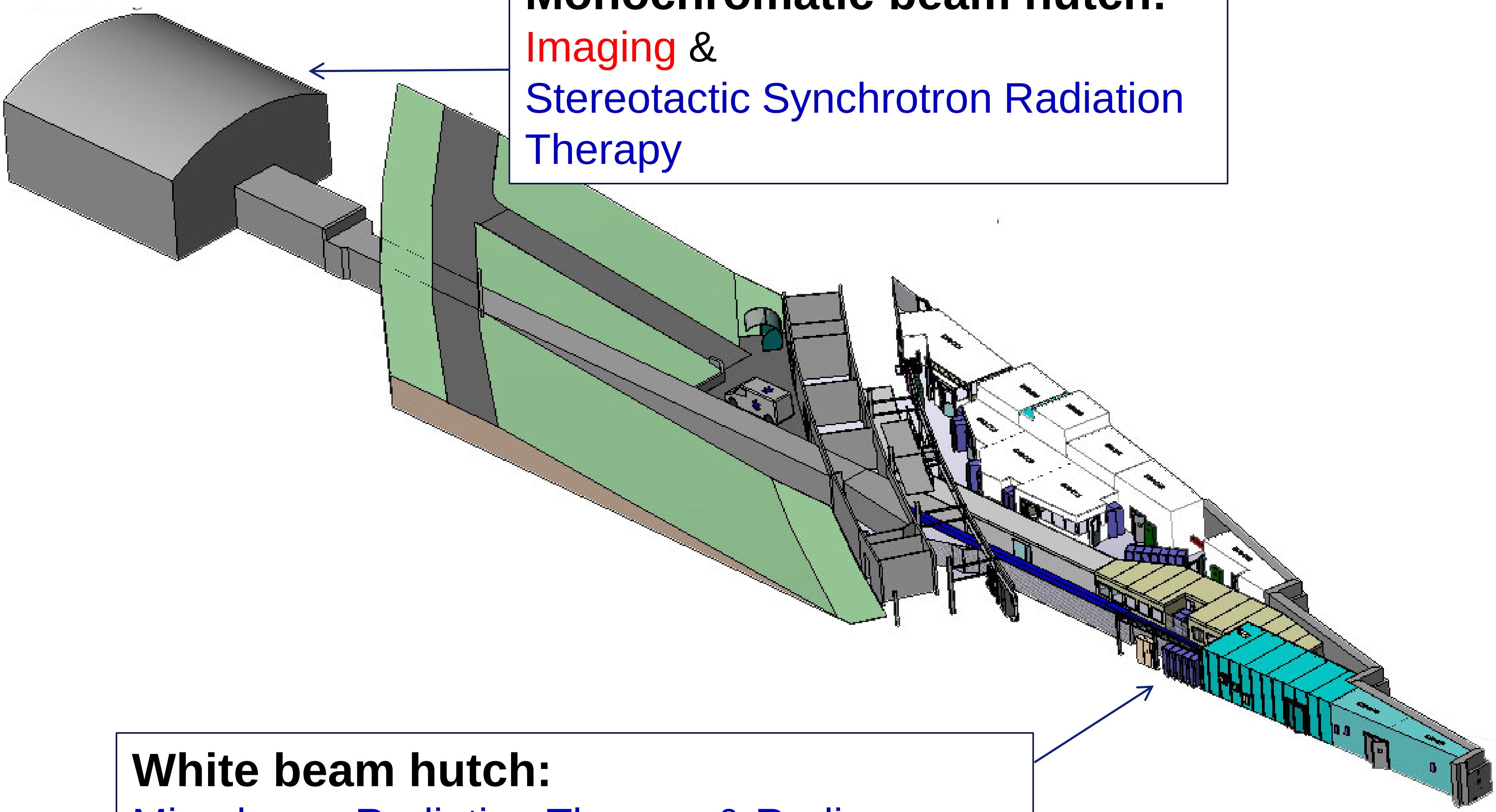

White beam hutch:
Microbeam Radiation Therapy & Radiosurgery

Lightning on the ESRF, 2002

ACKNOWLEDGMENTS

LMU, Munich

Paola Coan
Giacomo Barbone
Johannes Stroebel
Emamnuel Brun

University of Milano-Bicocca

Guido Cavaletti
Cecilia Ceresa
Gabriella Nicolini
Sara Semperboni

Consiglio Nazionale delle Ricerche
Istituto di Bioimmagini e Fisiologia Molecolare

Gabriele Biella
Antonio Zippo

ESRF

Alberto Mittone
Veronica Del Grosso
Peter Cloetens
Alexandra Pacureanu
Herwig Requardt

University of Padova

Valentina Gandin

CNR NANOTEC Institute of Nanotechnology
Centro Fermi

Alessia Cedola
Michela Fratini
Lorenzo Massimi
Francesco Brun

THANK YOU FOR YOUR ATTENTION